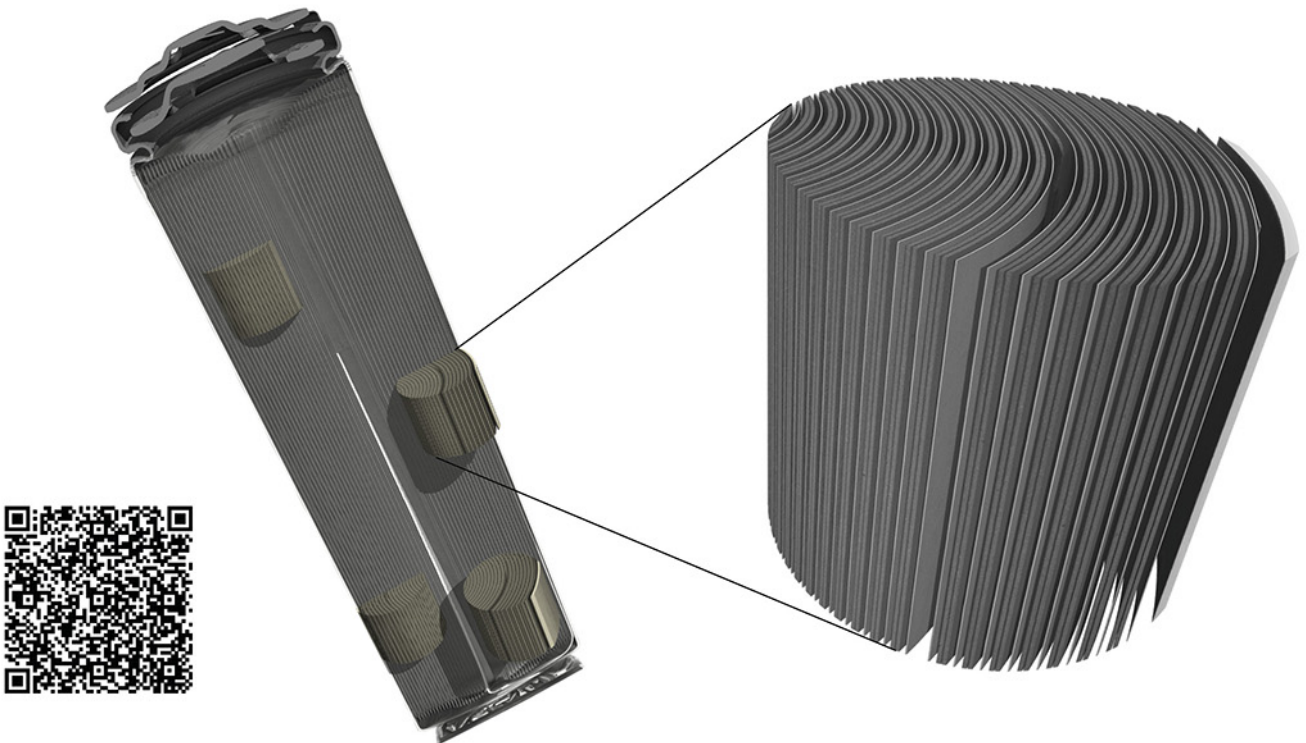


# TESCAN micro-CT solutions

## for energy storage materials research



## TESCAN UniTOM XL

- ✓ Multi-scale non-destructive 3D imaging optimized to maximize throughput and contrast
- ✓ Fast scanning and high sample throughput with temporal resolutions below 10 seconds
- ✓ Wide array of samples types
- ✓ Enables dynamic tomography and *in-situ* experiments
- ✓ Dynamic screening for synchrotron beamtime
- ✓ Modular and open system with unmatched flexibility for research



[Click and find out more](#)

# Open Framework Material Based Thin Films: Electrochemical Catalysis and State-of-the-art Technologies

Wei jin Li, Soumya Mukerjee, Baohui Ren, Rong Cao,\* and Roland A. Fischer\*

Open framework materials (OFMs), such as metal-organic frameworks and covalent organic frameworks have emerged as promising electrocatalysts to address the global energy crisis and environmental problems. Powdered non-film forms, that is, bulk OFMs exhibit excellent catalytic activities toward electrocatalytic carbon dioxide reduction, water splitting, and the oxygen reduction reaction. However, electrode preparation using bulk solids suffers from a range of oft-encountered difficulties, primarily limited by challenges in controlling their thickness, roughness, and particle sizes, despite early performance promises. Targeting energy sustainability, it is a matter of growing interest to directly integrate OFMs in the form of thin films onto conductive substrates. In essence, this leads to electrocatalysts with controlled features: thickness, roughness, and particle sizes. Thus far, there are only a handful of OFM thin films developed for electrocatalysis. Exploration of these understudied OFM thin films to serve electrocatalysis still lies at its infancy. This review will cover the key discoveries of OFM thin films as electrocatalysts and will critically examine the strengths, challenges, and future goals in exploring bespoke OFM thin films for electrocatalysis, under conditions that mimic real-world applications.

The production of renewable fuels from low-energy chemicals, such as water and CO<sub>2</sub>, is one promising avenue to ease the consumption of fossil fuels and to mitigate greenhouse gas production.<sup>[4,5]</sup> Nonetheless, water and/or CO<sub>2</sub> driven successful production of renewable fuels requires the combination of charge transfer and a fuel-forming catalytic reaction. One of the most important challenges in exploiting this economically attractive renewable energy resource is the development of highly active and robust catalysts that can facilitate H<sub>2</sub>O oxidation to molecular O<sub>2</sub> and H<sub>2</sub> or enables the transformation of CO<sub>2</sub> to useful fuels. A plethora of research efforts have recently boosted the development of CO<sub>2</sub> reduction and water oxidation electrocatalysts.<sup>[6–8]</sup> Albeit this impressive progress, there prevails a need to develop more advanced, better-performing, and low-cost electrocatalysts capable to manifest top-notch charge transport properties. Thanks to an assortment of positive factors such

## 1. Introduction

Ever-increasing fossil fuel combustion poses a global threat of the highest order to mankind contributing unfavorably to the global energy crisis and environmental issues such as, global warming, ocean acidification, drinking water scarcity, etc.<sup>[1–3]</sup>

as, the high density of surface active centers, earth-abundance, good stability, as well as reproducibility and an easy access to the active sites amenable to controlled design, etc., new-generation electrocatalysts are primed to address the pressing challenge of energy sustainability for a greener tomorrow.

Open framework materials (OFMs),<sup>[9,10]</sup> including metal-organic frameworks (MOFs),<sup>[11,12]</sup> covalent organic frameworks (COFs),<sup>[13,14]</sup> hybrid coordination networks,<sup>[15]</sup> porous aromatic frameworks (PAFs)<sup>[16]</sup> polymers of intrinsic microporosity (PIMs),<sup>[17]</sup> hyper-crosslinked polymers (HCPs),<sup>[18]</sup> and conjugated microporous polymers (CMPs),<sup>[19]</sup> have emerged as promising electrocatalysts, thanks to their abundant functions derived from a unique combination of properties such as tailored chemical functionality, high surface areas, uniform porosity, and well-defined periodic structures (**Figure 1**). Compared to the recently developed noble metal and transitional metal based inorganic electrocatalysts, OFMs offer key advantages as electrocatalysts. i) The primary advantage lies in the unique demonstration of two-in-one: both compositional modularity and tailored chemical functionality provide chemically tailored platforms and families, wherein the well-regulated electrochemical activities enable superior control over the number of active sites. For example, the coordination of benzimidazolone motifs to metal centers can facilitate proton-coupled electron transfer and result in the water oxidation catalysts reacting with water to form high-valent metal-oxo species at low potentials, avoiding high-energy intermediates.<sup>[20]</sup>

Dr. W. J. Li, Dr. S. Mukerjee, Prof. R. A. Fischer  
Chair of Inorganic and Metal-organic Chemistry & Catalysis Research Center  
Technical University of Munich  
Lichtenbergstr. 4 & Ernst-Otto-Fischer-Str. 1, 85748 Garching bei  
München, Germany  
E-mail: roland.fischer@tum.de

B. H. Ren, Prof. R. Cao  
State Key Laboratory of Structural Chemistry  
Fujian Institute of Research on the Structure of Matter  
Chinese Academy of Sciences  
Fuzhou 350002, P. R. China  
E-mail: rcao@firms.ac.cn

 The ORCID identification number(s) for the author(s) of this article can be found under <https://doi.org/10.1002/aenm.202003499>.

© 2021 The Authors. Advanced Energy Materials published by Wiley-VCH GmbH. This is an open access article under the terms of the Creative Commons Attribution-NonCommercial-NoDerivs License, which permits use and distribution in any medium, provided the original work is properly cited, the use is non-commercial and no modifications or adaptations are made.

DOI: 10.1002/aenm.202003499

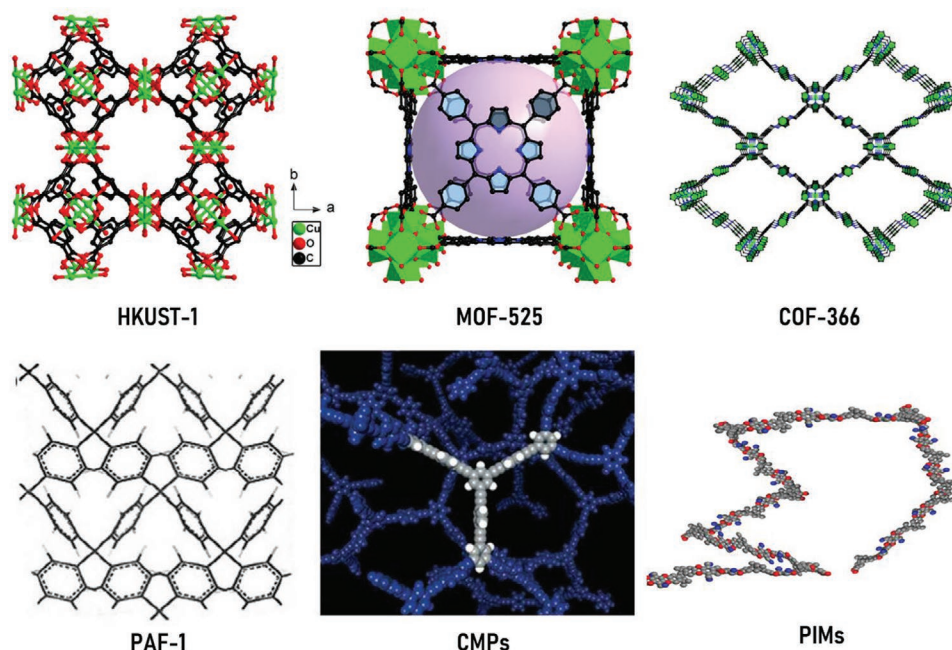


**Figure 1.** Schematic illustrations of a few representative families of OFMs. PAF-1. Reproduced with permission.<sup>[16]</sup> Copyright 2009, Wiley-VCH Verlag GmbH & Co. KGaA, Weinheim; CMPs. Reproduced with permission.<sup>[19]</sup> Copyright 2005, Wiley-VCH Verlag GmbH & Co. KGaA, Weinheim.

This investigation indicates that the inorganic and/or organic components in OFMs can act as synergistic catalysts in  $O_2$  evolving systems. Keeping this in mind, X. C. Wang and co-workers developed Co-ZIF-9 to catalyze water oxidation.<sup>[21]</sup> The quantum-chemical and electrochemical studies confirmed that incorporation of Co(II) and benzimidazole into MOFs can lead to enhanced water oxidation performances. ii) OFMs feature large surface areas and uniform porosity that prevent active sites from aggregation. This in turn increases density of the exposed catalytic centers selectively enabling a higher efficiency from the accessible sites. For example, drop-casting ultrathin NiCo bimetal-organic framework nanosheets on glassy-carbon (GC) electrodes were reported to exhibit high electrocatalytic activity for the oxygen evolution reaction (OER).<sup>[22]</sup> On the other hand, COFs as another subclass of OFMs, have been identified as promising lead candidates for electrocatalysis. Benefitting from their ordered structures, well-accessible functionalized pore walls, and tunable electrical properties, COFs enable researchers to precisely manipulate the spatial arrangement of catalytic centers within the predetermined 3D COF architectures, alongside offering their amenability to multivariate synthesis. Based on this approach of multivariate synthesis, topologically identical and functionally tailored building blocks can be introduced into the custom-built structures, a type of molecular Lego.<sup>[13]</sup> The intrinsic characteristics of COFs can potentially combine the merits of molecular and heterogeneous catalysts.<sup>[23]</sup> iii) Long-range order in the heterogeneous porous framework not only allowed the free permeation of electrolyte counterions and dissolved  $CO_2$ , water and/or  $O_2$  into the film interior, but could also be utilized to immobilize molecular catalysts (e.g., metal porphyrins) to avoid aggregation and deactivation processes. iv) OFMs are usually formed by low-cost and earth-abundant transitional metals and/or inexpensive organic ligands/compounds,

promoting their widespread applications in renewable energy technologies.

OFMs find their most use in bulk form. In general, to serve electrocatalysis, the OFMs need to be integrated onto conductive solid substrates. A typical preparative method involves drop-casting the bulky OFM powders onto a suitable electrode surface as the coating for electrocatalysis. However, thickness and morphology of the as-prepared OFM coatings are difficult to be controlled once the electrode surface is coated by drop-casting. Additionally as a binder, Nafion is needed to post-synthetically treat the OFM layers via drop-casting.<sup>[24]</sup> At this point, densities of the coordinatively unsaturated active metal sites available to the catalytic substrate are physically obscured by the Nafion. Thus, studying the growth of OFM films directly onto the electrode is a topic of increasing relevance. Development of OFMs directly onto the electrodes in the form of electrocatalytically active thin films is an understudied area of research with a lot of promises ahead. Many challenges remain unmet regarding the fabrication and characterization of OFM thin films as well as the development of OFM thin films as efficient electrocatalysts.

Compared to drop-casting, growing OFMs directly onto conductive substrates as thin films offers the following prime advantages:<sup>[25–28]</sup> i) First, the as-prepared OFM thin films allow their direct use as electrode without the need for any time-consuming post-deposition. ii) In addition, the as-prepared films can attach tightly to the electrode surface. The OFM films are directly anchored on solid surface by chemical bonds of diverse nature (e.g., coordination bonds, hydrogen bonds, intermolecular forces, etc.) avoiding unobstructed access to the respective pore cavities. iii) Furthermore, it allows fine-tuning the thickness and morphology during deposition processes of thin films, which influences electron and charge transfer rates. Consequently, this affects electrocatalytic efficiency.

iv) Integrating OFMs as thin films will maximize the surface-active sites without the need to be shielded by Nafion or other similar conductive sealing agents. The large surface areas of OFMs can offer high density of catalytic sites with precise spatial arrangement of the reactant. v) Porosity of the OFMs allows an unrestricted transport of the participating guest molecules to increase the thermal and chemical tolerances of their intermediates, exemplifying embedded active catalysts. iv) Some OFMs also display characteristics that are favorable for capture and transport of electrons, including their modular composition that comprise electronically tunable organic linkers, adjustable band gaps, and extended networks.

Herein, contextualizing the challenges involved, we discuss the advances of using OFM films as electrochemical catalysts. The state-of-the-art in OFM films for electroanalysis is overviewed. Secrets behind choosing the deposition methods and challenges to develop OFM films for well-defined electrodes are discussed. Last but not the least, we critically examine the development of OFM films as electrocatalysts on conductive substrates, centered around the current handicaps. In our and others cohesive attempts to overcome these limitations, the status quo on understanding the holistic behavior of OFM films as electrochemical catalysts will be greatly improved. In principle, these collective understandings can be leveraged to elevate the OFM derived electrocatalytic efficiencies. This perspective not only aims to provide readers with a comprehensive knowledge on the foregoing topic by providing updates on the latest progress, but also puts forward futuristic design principles around this class of materials.

## 2. State-of-the-art in OFM Thin Films with Various Dimensionality for Electrocatalysis

Electrocatalysts play a key role in lowering overpotentials, increasing reaction kinetics, efficiency, and selectivity of the chemical transformations.<sup>[6,29]</sup> They are known to act as electron transfer agents that ideally provide the driving force in the reactions happening at the thermodynamic potential,  $E^0_{(\text{products/substrates})}$ . At a given current density, there always exists a difference between the applied electrode potential,  $V_{\text{applied}}$ , and  $E^0_{(\text{products/substrates})}$ , referred to as overpotential. Direct electrochemical transformations on most electrode surfaces need large overvoltages to trigger the reactions, lowering the conversion efficiency and selectivity as a direct outcome. To lower overvoltages and improve the efficiency, the design of electrocatalysts need to focus upon formal potentials,  $E^0_{(\text{Cat}^{n+/0})}$  in close match to  $E^0_{(\text{products/substrates})}$ , and elevated kinetic rate constants, for the chemical transformation of substrates to products to occur at this potential (Figure 2). In this section, the state-of-the-art in OFM thin film based electrocatalysts are discussed. These include clean energy relevant reactions such as,  $\text{CO}_2$  reduction, hydrogen ( $\text{H}_2$ ) evolution, and  $\text{O}_2$  reduction/evolution. The key structure-property relationships with respect to electrocatalytic activities of the hitherto published OFM thin films and derived composites will be deciphered, offering insights into the design principles that can potentially lead mankind to greener energy-sustainable alternatives of the future. Generally elucidating, four paths have been reported on

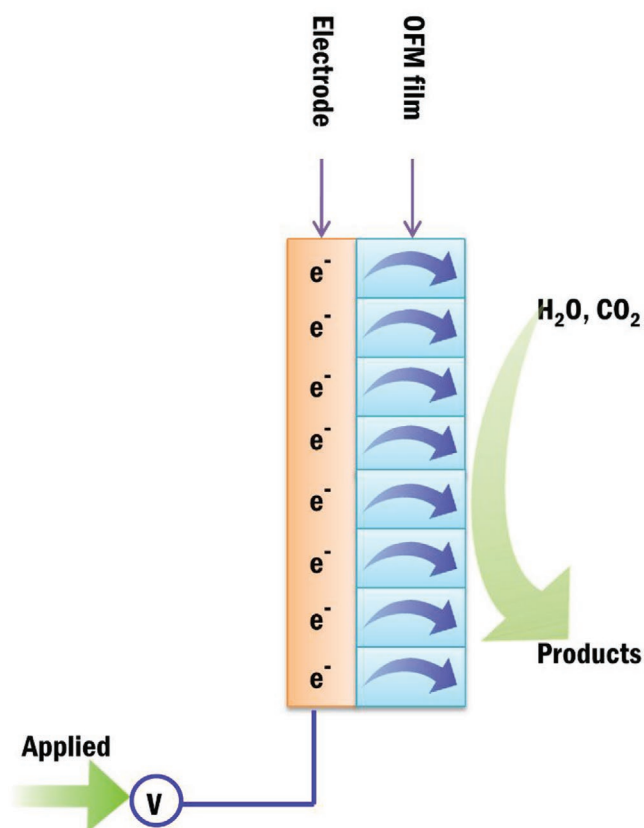


**Figure 2.** Schematic illustration of electrocatalysis with a model electron source transferred by electrocatalysts.

the use of OFM films as electrocatalysts: i) embedding active sites into the pores and/or building units of OFMs; ii) OFMs' building units directly function as active sites; iii) OFMs offer as a reservoir for adsorbing reactants and diffusing products; iv) OFM films act as precursors to derive the active sites.

### 2.1. Electrocatalytic OFM Thin Films Involved in $\text{CO}_2$ Reduction

Electrochemical  $\text{CO}_2$  reduction is a multi-electron transfer reaction. Depending on the structure and morphology of OFM electrode materials and electrolytes, the products of  $\text{CO}_2$  reduction are carbon monoxide (CO) and formic acid, formaldehyde, methanol ( $\text{CH}_3\text{OH}$ ), or methane (Table 1).

The reaction pathways were primarily determined by experimental parameters, such as electrolytes, species of catalysts, potentials, and so on. The completely catalytic reaction process mainly contains three steps:<sup>[4,30]</sup> i)  $\text{CO}_2$  surface adsorption; ii) combination and transformation of  $\text{CO}_2$  with electron and proton; iii) the release of products. To be specific, the catalysts perturb the  $\text{C}=\text{O}$  bond as soon as  $\text{CO}_2$  adsorbs on the heterogeneous catalysts surface. This perturbing  $\text{C}=\text{O}$  bond stage is the most essential step in the whole reaction process. During this process, the electrons and protons are shared between  $\text{CO}_2$  and the catalysts. This gets transferred to  $\text{CO}^*$  ( $\text{CO}_2$  in aqueous media) and further hydrogenation occurs to form  $\text{COOH}^*$  ( $\text{HCO}_2^*$ ) in electron-proton system (\* refers to a site

**Table 1.** Possible half reactions of CO<sub>2</sub> reduction associated with multi-electron transfer. (Normal hydrogen electrode (NHE), 25 °C, pH 7).<sup>[6]</sup>

Reactions	Theoretical potential [V vs NHE]
CO <sub>2</sub> + 2H <sup>+</sup> + 2e <sup>-</sup> → CO + H <sub>2</sub> O	-0.52
CO <sub>2</sub> + 2H <sup>+</sup> + 2e <sup>-</sup> → HCO <sub>2</sub> H	-0.61
CO <sub>2</sub> + 4H <sup>+</sup> + 4e <sup>-</sup> → HCHO + H <sub>2</sub> O	-0.51
CO <sub>2</sub> + 6H <sup>+</sup> + 6e <sup>-</sup> → CH <sub>3</sub> OH + H <sub>2</sub> O	-0.38
CO <sub>2</sub> + 8H <sup>+</sup> + 8e <sup>-</sup> → CH <sub>4</sub> + 2H <sub>2</sub> O	-0.24
2CO <sub>2</sub> + 8H <sub>2</sub> O + 12e <sup>-</sup> → C <sub>2</sub> H <sub>4</sub> + 12OH <sup>-</sup>	-0.34
CO <sub>2</sub> + 2e <sup>-</sup> → 2CO <sup>-</sup>	-1.9

on catalysts/electrode surface). Depending on the binding ability of the catalysts with CO\* and COOH\* intermediates, CO<sub>2</sub> converts to different products and thereafter desorbed. For instance, in the case of weak adsorption capacity of catalysts for CO and strong binding with COOH\*, CO<sub>2</sub> tends to be reduced to CO. Or else, it will be further reduced to other products. Unlike electron-proton reaction systems, in aprotic solvents such as DMF, the reaction tends to dimerize the two carbon radical anions (CO<sub>2</sub><sup>-</sup>). In other words, the generated CO<sub>2</sub><sup>-</sup> tends to react with another adsorbed CO<sub>2</sub> molecule in nonaqueous (CO<sub>2</sub><sup>-</sup> + CO<sub>2</sub> → O<sub>2</sub>C-CO<sub>2</sub><sup>-</sup>). It is worth noting that various mechanisms within different catalysts might coexist. For clarity, herein we limit our discussion only to the widely accepted mechanisms.

Hupp and co-workers built a test system by depositing Fe-MOF-525, built from Fe(II)-porphyrin units and Zr(IV), onto a FTO surface.<sup>[31]</sup> The resulting thin film displayed a high surface concentration of catalytic active sites, approximately three orders of magnitude higher to the estimated catalyst monolayer. Besides, the as-prepared MOF thin films revealed close to one order of magnitude higher performance versus all previously reported molecular catalysts examined for CO<sub>2</sub> reduction. These studies demonstrate that the Fe-MOF-525 films could transfer charge/electrons via a redox hopping path between the neighboring Fe-TCPP sites (**Figure 3**). Under electrical environment, Fe(I/0) could be produced from the Fe-MOF-525 films, catalyzing the reduction of CO<sub>2</sub> to CO and H<sub>2</sub> with Faradaic efficiencies (FE) of 54 ± 2% and 45 ± 1%, respectively. These results are suggestive of superior catalytic efficiencies in bulk phase, comparable to observations in homogeneous electrocatalysis. Morris et al. detailed that the catalytic ability of metal-porphyrin based MOF thin films contribute to their observed

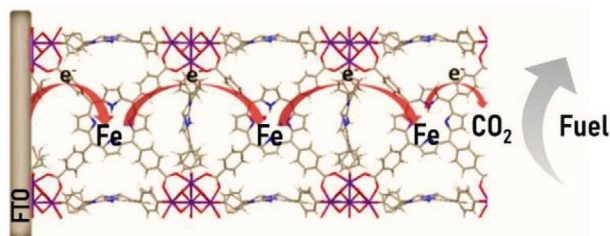


**Figure 3.** Schematic representation of a typical hopping mechanism in MOF-525, catalyzing CO<sub>2</sub> reduction. Reproduced with permission.<sup>[31]</sup> Copyright 2015, American Chemical Society.

performance.<sup>[40]</sup> The observed charge transport was ascribed to redox hopping mechanism, which further translated to the associated reduction efficiency. Sun et al. developed a highly oriented Re-SURMOF thin film for CO<sub>2</sub> reduction.<sup>[34]</sup> DFT calculations revealed a more efficient charge transfer along the crystallographic [001] direction. However, electrical conductivities of the prepared thin films were not measured. These results demonstrate that the porous architectures in OFMs play a key role in concentrating CO<sub>2</sub> on the resulting electrode surface and to increase the number of active sites therein.

Besides MOF thin film-modified electrodes/electrocatalysts, ingenious choice of electrolytes is also crucial in electrocatalysis. Different electrodes and electrolytes can produce electrochemical assemblies of varying natures. Han and co-workers conducted a study of electrochemical CO<sub>2</sub> reduction by the combination of Zn-BTC MOF thin films as electrode and ionic liquids (ILs) as electrolytes.<sup>[32]</sup> A series of CO<sub>2</sub> reduction experiments were carried out in CO<sub>2</sub>-saturated 1-butyl-3-methylimidazolium tetrafluoroborate (BmimBF<sub>4</sub>). The evidences obtained from CPE experiments suggested that the as-prepared Zn-BTC MOF thin films and ILs could synergistically and selectively reduce CO<sub>2</sub> to CH<sub>4</sub> with a FE higher than 80.1 ± 6.6%. The high reduction efficiencies are credited to the amalgamation of ILs and Zn-BTC MOF thin films. Upon immersing the Zn-BTC film in the IL electrolytes, imidazolium cations can assist in concentrating CO<sub>2</sub> near the film surface. CO<sub>2</sub> was converted into molecular CO when the electrons were transferred by Zn-MOF films. Zn-MOF features a larger adsorption capacity of CO than CH<sub>4</sub>, thus the CO molecules were preferentially adsorbed on Zn-MOF film surface, to be converted into CH<sub>4</sub>.

As another class of OFM films, COF films have been developed for catalytic CO<sub>2</sub> reduction. Alike other OFMs, COF films are not just limited to precise manipulation of catalytic centers arranged spatially within the predetermined COF structures by expanding and functionalizing the frameworks without changing their underlying structures. Fine-tuning the COF pore environment, both sterically and electronically around the active sites is an allowed feature herein, by offering ready access to the substrate. Keeping these in mind, Yaghi and co-workers incorporated cobalt(II) porphyrin units into COFs, together with multivariate synthesized frameworks composed of catalytic Co(II) sustained by the Cu(II)framework, generating a highly stable and selective catalyst for electrochemical CO<sub>2</sub> reduction to CO.<sup>[23]</sup> Its catalytic activity on CO<sub>2</sub> reduction underwent an increase when compared to the Co(I)-COFs. The FE for CO was 90 % in CO<sub>2</sub> saturated aqueous bicarbonate buffer (pH = 7) at -0.67 V versus a reversible hydrogen electrode (RHE). These results indicate that the as-prepared COF-366-Co exhibited high selectivity over competing proton reduction. The catalytic efficiencies could be improved via framework expansion by functionalizing the constituent organic ligands. Additionally, isostructural metalloporphyrin units were introduced to dilute electroactive cobalt porphyrin active sites within the extended framework to enhance the number of exposed active sites in the reactant and to further improve the turnover frequency on a per-cobalt basis. The results show that the TOF increased with a decrease in Co/Cu ratio, suggesting that multivariate Co/Cu COF-367 catalysts could perform substantially better by introducing two transition metals into each unit of

**Table 2.** State-of-the-art OFM based thin films used for electrocatalytic CO<sub>2</sub> reduction.

OFM films	Support	Deposition method	Potential	Main Product	FE [%]	Refs.
MOF-525	FTO	Electrophoresis	-1.3 V versus NHE	CO	54 ± 2	[31]
Zn-BTC	Carbon paper	Electrophoresis	-2.2 V versus Ag/Ag <sup>+</sup>	CH <sub>4</sub>	> 80	[32]
COF-366	FTO	Solvothermal method	-0.55 V versus RHE	CO	> 90	[23]
Al <sub>2</sub> (OH) <sub>2</sub> TCPP-Co	Carbon disk	ALD and microwave	-0.7 V versus RHE	CO	76	[33]
ReL(CO) <sub>3</sub> Cl (L = 2,2'-bipyridine-5,5'-dicarboxylic acid)	FTO	LBL	-1.6 V versus NHE	CO	93	[34]
ZIF-8 Cu(bdc) <sub>x</sub> H <sub>2</sub> ORE-ndc-fcu-MOF Al-TCPP	Au microelectrode	LBL	-0.5 V versus RHE	CH <sub>4</sub> and C <sub>2</sub> H <sub>4</sub>	56	[35]
Co@NU-1000	FTO	Solvothermal method	-0.82 V versus RHE	CO and HCOOH	6 (CO); 28 HCOOH	[36]
Ag@Al-PMOF	GC	ALD and microwave reactor	-1.1 V versus RHE	CO	55.8	[37]
MFM-300(In)	Indium foil	Electrochemical deposition	-2.15 V versus Ag/Ag <sup>+</sup>	HCOOH	99.1	[38]
FeDhaTph-COF	Carbon cloth	Solvothermal method	-2.2 V versus Ag/Ag <sup>+</sup>	CO	80	[39]

UU: Uppsala University; ndc = 1,4-naphthalenedicarboxylic acid; TCPP = tetrakis(4-carboxyphenyl)-porphyrin; <sup>r</sup>SURMOF: surface-mounted MOF; x = -Br, -OCH<sub>3</sub>, -H, -NH<sub>2</sub>; ALD = atomic layer deposition.

the COFs. However, the FE of CO production took a downturn with the decrease of Co/Cu ratio due to the moderate proton reduction ability of the copper porphyrin sites within the hybrid organic framework.

The aforementioned products produced by electrocatalytic CO<sub>2</sub> reduction of the OFM films are mainly gases such as CO, CH<sub>4</sub>, C<sub>2</sub>H<sub>4</sub> or HCOOH (Table 2). Utilization of OFM films for electrochemically reducing CO<sub>2</sub> to alcohol is still in its infancy. Electrochemical conversion of CO<sub>2</sub> to valuable liquid products (e.g., methanol and ethanol) remains a challenge since this requires a large overpotential and is kinetically slower with 6- or 12-electron transfer. Some bulk MOFs, such as HKUST-1 and Ru doped HKUST-1 are reported to electrochemically produce methanol and ethanol.<sup>[41,42]</sup> However, both HKUST-1 variants suffer from low FE and low stability for long reactions. To boost the yield of liquid products, strong binding sites with the CO intermediate act as key factors in electrocatalysis, suppressing

the deoxygenation of HOCCH intermediates.<sup>[43,44]</sup> To this end, hydroxide doped or heteroatom (e.g., S, N, and B) doped Cu(II) OFM based thin films appear viable candidates in terms of producing the desired liquid products of electrochemical CO<sub>2</sub> reduction.<sup>[45-47]</sup>

## 2.2. Electrocatalytic OFM Thin Films that Promote Water Splitting and Oxygen Reduction Reaction

In all likelihood, water is a limitless resource, especially if the vastly untapped resource of sea-water can be used. Development of efficient water splitting is a critical advance to generate clean fuels (e.g., H<sub>2</sub>). Once a sufficient overpotential is applied, water is possible to get reduced to H<sub>2</sub> and oxidized to O<sub>2</sub>, respectively, by installing corresponding catalysts on cathode and anode (Figure 4). Thus, electrocatalytic devices for water

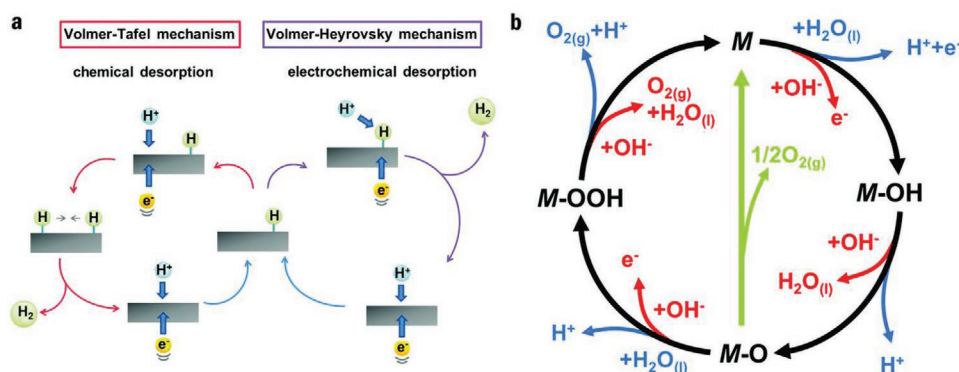


**Figure 4.** Schematic illustration of a) the hydrogen evolution mechanism in acidic media. Reproduced with permission.<sup>[48]</sup> Copyright 2014, Royal Society of Chemistry. b) The OER mechanisms at a solid electrode for acidic (blue line) and alkaline (red line) electrolytes. The black line indicates that the oxygen evolution involves the formation of a peroxide (M-OOH) intermediate (black line) while another route for direct reaction of two adjacent oxo (M-O) intermediates (green) to produce oxygen is possible as well. Reproduced with permission.<sup>[50]</sup> Copyright 2017, Royal Society of Chemistry.

splitting are composed of suitable catalysts supported on an anode electrode, or catalysts tethered on a cathode electrode, offering a relatively straightforward approach to harness the catalytic current from a suitable heterogeneous material.

A myriad of energy and environmental concerns caused by fossil fuel consumption are increasing. In this context, the developing landscape of renewable and sustainable energy management has evolved from “burning fossil fuels” to “green energy conversion”, thanks to the latter demonstrating higher efficiency and eco-friendliness. Therefore, development of effective conversion technologies is of high importance. One of the promising energy conversion device featuring clean emissions and high-energy conversion efficiency is exemplified by fuel cells, which is oft-employed as power sources for electronics, mobiles, and other portable devices. Directly controlling the overall efficiency of a fuel cell, the underlying process of oxygen reduction reaction (ORR) plays a key role. Therefore, development of low-cost, earth-abundant, and highly stable ORR electrocatalysts is of topical prominence to achieve new benchmark efficiencies, paving the ways for widespread applications of fuel cells.

Electrocatalytic water splitting comprises two half-reactions, one each of hydrogen evolution reaction (HER) and OER. HER is a two electron transfer reaction (Table 3). In acidic media, it is a multi-step process occurring on the electrode surface (Figure 4 and equations 1–4). In the first step, an adsorbed hydrogen atom is produced by transferring an electron to the interface whereas one proton is adsorbed at the electrocatalyst surface (Equation 2). The step that provides adsorbed hydrogen atom is also denoted as Volmer or discharge reaction. Following the Volmer reaction, there are two possible reaction pathways: one is the Heyrovsky step (equation 3) while the other is Tafel step (equation 4). Both depends on the applied potential and the nature of electrocatalyst surface.<sup>[51]</sup> In alkaline media, these two widely accepted mechanisms of HER have been demonstrated by Equations 15–18.<sup>[52]</sup> Concerning the OER, it can be conducted under acidic as well as alkaline media. The possible mechanisms for the OER are shown in Figure 4b and Table 3, equations 5–11, 19–24.

Conversely in the ORR, it can occur in acidic as well as alkaline media via two- or four-electron transfer pathways. In principle, the two-electron transfer pathway affords peroxide species as an intermediate, further reducing the intermediate to H<sub>2</sub>O/OH<sup>-</sup> (Table 3, equations 13, 14 and equations 26, 27). The four-electron transfer pathway reduces oxygen directly to H<sub>2</sub>O/OH<sup>-</sup> (Table 3, equations 12 and 25). According to the mechanisms of HER, OER, and ORR, density of the catalytically active sites, binding strengths in the reaction intermediates and the conductivity of electrocatalysts allude to be the key parameters in the design of efficient catalysts.

So far, only a handful of OFM films have been utilized for electrocatalytically driven water reduction and oxidation processes (Table 4).<sup>[65]</sup> Hupp and co-workers mounted catalytically active Co(II) ions and Ni–S on the thin film surface of MOF NU-1000.<sup>[54,56]</sup> The pre-prepared NU-1000 MOF thin films are composed of spatially arranged sub-micrometer rods, serving as a scaffold for anchoring areal density of the Co-catalyst sites. The Co-catalyst sites are likely tethered to the nodes of NU-1000. In this case, the deposited thin films revealed

**Table 3.** Mechanisms of HER, OER, and ORR.<sup>[48–50]</sup>

In acidic media (“M” is denoted as a site on the catalyst surface)	
HER: 2H <sup>+</sup> + 2e <sup>-</sup> → H <sub>2</sub>	(1)
H <sub>3</sub> O <sup>+</sup> + M + e <sup>-</sup> → M – H <sub>ads</sub> + H <sub>2</sub> O (Volmer step)	(2)
M – H <sub>ads</sub> + H <sub>3</sub> O <sup>+</sup> + e <sup>-</sup> → M + H <sub>2</sub> + H <sub>2</sub> O (Heyrovsky step)	(3)
2M – H <sub>ads</sub> → H <sub>2</sub> + 2M (Tafel step)	(4)
OER: 2H <sub>2</sub> O → O <sub>2</sub> + 4H <sup>+</sup> + 4e <sup>-</sup>	(5)
M + H <sub>2</sub> O → M – OH <sub>ads</sub> + H <sup>+</sup> + e <sup>-</sup>	(6)
M – OH <sub>ads</sub> → M – O <sub>ads</sub> + H <sup>+</sup> + e <sup>-</sup>	(7)
2M – O <sub>ads</sub> → 2M + O <sub>2</sub>	(8)
M – O <sub>ads</sub> + H <sub>2</sub> O → M – OOH <sub>ads</sub> + H <sup>+</sup> + e <sup>-</sup>	(10)
M – OOH <sub>ads</sub> + H <sub>2</sub> O → M + O <sub>2</sub> + H <sub>3</sub> O <sup>+</sup> + e <sup>-</sup>	(11)
ORR: O <sub>2</sub> + 4H <sup>+</sup> + 4e <sup>-</sup> → 2H <sub>2</sub> O (Four-electron pathway)	(12)
O <sub>2</sub> + 2H <sup>+</sup> + 2e <sup>-</sup> → H <sub>2</sub> O <sub>2</sub> (Two-electron pathway)	(13)
H <sub>2</sub> O <sub>2</sub> + 2H <sup>+</sup> + 2e <sup>-</sup> → 2H <sub>2</sub> O	(14)
In alkaline media	
HER: 2H <sub>2</sub> O + 2e <sup>-</sup> → H <sub>2</sub> + 2OH <sup>-</sup>	(15)
2H <sub>2</sub> O + 2e <sup>-</sup> → 2H <sub>ads</sub> + 2OH <sup>-</sup> (Volmer step)	(16)
H <sub>2</sub> O + H <sub>ads</sub> + e <sup>-</sup> → H <sub>2</sub> + OH <sup>-</sup> (Heyrovsky step)	(17)
2H <sub>ads</sub> → H <sub>2</sub> (Tafel step)	(18)
OER: 4OH <sup>-</sup> → 2O <sub>2</sub> + 2H <sub>2</sub> O + 4e <sup>-</sup>	(19)
M + OH <sup>-</sup> → M – OH <sub>ads</sub> + e <sup>-</sup>	(20)
M – OH <sub>ads</sub> + OH <sup>-</sup> → M – O <sub>ads</sub> + H <sub>2</sub> O + e <sup>-</sup>	(21)
2M – O <sub>ads</sub> → 2M + O <sub>2</sub>	(22)
M – O <sub>ads</sub> + OH <sup>-</sup> → M – OOH <sub>ads</sub> + e <sup>-</sup>	(23)
M – OOH <sub>ads</sub> + OH <sup>-</sup> → M + O <sub>2</sub> + H <sub>2</sub> O + e <sup>-</sup>	(24)
ORR: O <sub>2</sub> + 2H <sub>2</sub> O + 4e <sup>-</sup> → 4OH <sup>-</sup> (Four-electron pathway)	(25)
O <sub>2</sub> + H <sub>2</sub> O + 2e <sup>-</sup> → HO <sub>2</sub> <sup>-</sup> + OH <sup>-</sup> (Two-electron pathway)	(26)
HO <sub>2</sub> <sup>-</sup> + H <sub>2</sub> O + 2e <sup>-</sup> → 3OH <sup>-</sup>	(27)

improved electrochemical activity in terms of FE versus the reported bulk MOFs due to the increased number of active sites. In this respect, MOF thin films are used as a template to anchor and expose catalytic sites (Figure 5). Similarly, Ott and co-workers introduced cobaloxime hydrogen evolution catalyst linkers coordinated to inorganic nodes of zirconium-oxo cluster to form a new MOF UU-100(Co).<sup>[53]</sup> UU-100(Co) demonstrated a FE of 84% for hydrogen evolution, when fabricated as thin films. These reports confirm that both approaches of including catalytically active sites to the MOF pores of the thin film and including catalytically active sites to MOF struts could significantly improve their catalytic performances.

Meanwhile, Zhao and co-workers fabricated an ultrathin nanosheet array of NiFe-based MOF films on Ni foam.<sup>[57]</sup> The reported ultrathin NiFe-MOF films reveal a relatively high electronic conductivity of 1 ± 0.2 × 10<sup>-3</sup> S · cm<sup>-1</sup>. Moreover, Zhao et al. found that the direct growth of NiFe-MOF on conductive substrates display smaller contact resistance (2.8 Ω) than the conductive substrates (8.2 Ω) prepared by drop-casting bulk NiFe-MOF crystallites. These results suggest that the prepared NiFe-MOF films can exhibit dual merits of highly exposed

**Table 4.** State-of-the-art OFM based thin films used for electrocatalytic water splitting and ORR.

OFM films	Support	Deposition method	Reactant	Product	$\eta_{\text{onset}}^{\text{a)}$ [V vs RHE]	FE [%]	Refs.
UU-100(Co)	FTO	Solvothermal	H <sub>2</sub> O	H <sub>2</sub>	≈−0.15	84	[53]
NU-1000_Ni−S	FTO	Electrodeposition	H <sub>2</sub> O	H <sub>2</sub>	≈−0.11	93	[54]
Co/Ni(BDC) <sub>2</sub> TED	LBL	Ni foam	H <sub>2</sub> O	O <sub>2</sub>	0.16	98.3	[55]
Atomic Co coated NU-1000	FTO	Solvothermal with ALD of Co	H <sub>2</sub> O	O <sub>2</sub>	0.4	≈100	[56]
Ni−Fe MOF	Ni foam	Solvothermal	H <sub>2</sub> O	O <sub>2</sub> , H <sub>2</sub>	0.11	95	[57]
NiPc-MOF	FTO	Solvothermal	H <sub>2</sub> O	O <sub>2</sub>	0.25	94	[58]
NiFe-BTC	Ni foam	Electrochemical deposition	H <sub>2</sub> O	O <sub>2</sub>	0.17	95	[59]
NiCo-BDC SURMOF	Pt microelectrode	LBL	H <sub>2</sub> O	O <sub>2</sub>	≈0.15	99.4	[60]
NiFe-BDC(x) SURMOF	Au electrode	LBL	H <sub>2</sub> O	O <sub>2</sub>	≈0.18	Not given	[61]
Ni <sub>2</sub> (HITP) <sub>3</sub>	GC	Solvothermal	O <sub>2</sub>	H <sub>2</sub> O <sub>2</sub>	0.18 (vs Pt)	> 63	[62]
PCN-223 (Fe)	FTO	Solvothermal	O <sub>2</sub>	H <sub>2</sub> O/H <sub>2</sub> O <sub>2</sub>	−0.5 V versus NHE	34 for H <sub>2</sub> O <sub>2</sub>	[63]
Ni-THT	Rotating disk electrode	Langmuir Blodgett	H <sub>2</sub> O	H <sub>2</sub>	0.11	Not given	[64]

<sup>a)</sup>onset overpotential; UU: Uppsala University; ndc = 1,4-naphthalenedicarboxylic acid; TCPP = tetrakis(4-carboxyphenyl)-porphyrin; SURMOF: surface-mounted MOF; x = −Br, −OCH<sub>3</sub>, −H, −NH<sub>2</sub>; TED = triethylenediamine; Pc = phthalocyanine.

active molecular metal sites and improved conductivity. Hence, the NiFe-MOF films record an excellent electrocatalytic activity toward OER with a small onset overpotential of 110 mV (the overpotential at 10% of the peak current) and a small overpotential of 240 mV at 10 mA · cm<sup>−2</sup>.

On the other hand, Dincă and co-workers developed a prototypical conductive MOF, Ni<sub>3</sub>(HITP)<sub>2</sub> (HITP = 2,3,6,7,10,11-hexaiminotriphenylene) directly fabricated onto conductive substrates for the ORR.<sup>[62]</sup> Taking advantages of the electrical conductivity ( $\sigma = 40 \text{ S} \cdot \text{cm}^{-1}$ ), high surface area, and tunable chemical structure of Ni<sub>3</sub>(HITP)<sub>2</sub>, the as-prepared MOF films exhibit a small overpotential relative to Pt ( $E_{\text{onset}} = 1.0 \text{ V}$ ). At this point, the result indicates that Ni<sub>3</sub>(HITP)<sub>2</sub> film is the most active ORR electrocatalyst, notching activities in the same order of magnitude as the most active non-platinum metal electrocatalysts. That the direct deposition of MOF onto conductive substrates can enhance the catalyst-substrate contact on binder-free electrode to improve the efficiency of electron transport, resulting in high catalytic activity served as a fitting explanation to the observation.

In summary, OFM films and their derivatives have demonstrated their excellent electrocatalytic performances due to advantages they intrinsically derive from custom-designed

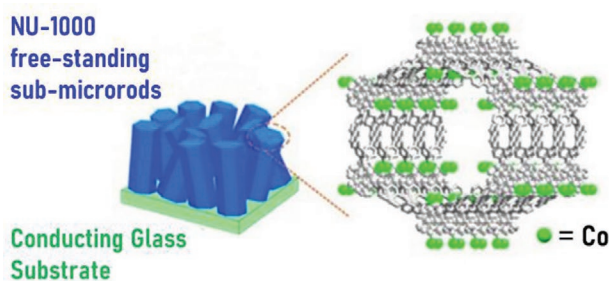


**Figure 5.** Schematic representation of 3D arrays of separated atomic Co(II) in NU-1000 thin film. Reproduced with permission.<sup>[56]</sup> Copyright 2015, American Chemical Society.

structural features and film fabrication. For example, the host OFMs can inherit the merits of well-defined/tunable chemical structures, high surface areas, and readily accessible active sites. The crystalline solid state of OFM films can offer a conveniently recyclable and robust matrix, resistant to chemical and physical treatments. Rational design of OFMs as thin films can maximize the exposure to active sites, improve the electron and mass transport, all consequently adding up to provide high catalytic activity. These custom-designed OFMs, upon synergizing with film fabrication diversities are primed to boost the expanding catalogue of electrocatalysts (Table 5). However, regarding electrocatalysis, current reports mainly focus on fabricating MOFs in the form of thin films, whereas COFs and other OFMs are hitherto unexplored. One plausible reason is the fact that COFs and other OFMs are not as easy as MOFs to be deposited as thin films directly onto conductive electrodes.

### 3. Deposition Techniques of OFM Film Based Materials Suited for Electrocatalytic Applications

It is worth noting that to neatly deposit OFMs onto the electrodes in the form of thin films is crucial to maximize electrocatalytic performances. The compatibility between OFMs and substrates holds a key issue in improving catalytic efficiency of the catalysts. The substrates where OFM thin films are deposited render great influence on the applications of these thin films.<sup>[66–69,75]</sup> Regarding electrocatalysis, catalysts are required to be deposited on conductive surfaces (e.g., metal plates, indium tin oxide (ITO) glass, FTO, glass and GC, etc.).<sup>[26]</sup> A wide variety of techniques and various substrates have been documented on fabricating OFM films, especially for the access of MOF films. However, in this perspective, greater attention is paid to the OFM films deposited on conductive substrates and their respective film fabrication techniques (Table 6). Besides, improving the crystallinity and porosity of the prepared OFM films comprise critical issues that need to be taken into



**Table 6.** Typical examples of various techniques to prepare OFM films on conductive substrates.

Substrates	OFM	Techniques	applications	Refs.
SAMs on Au	MOF-5	Solvothermal method Solvothermal method	Not given	[73]
	HKUST-1		Not given	[74]
SAMs on FTO	CoPIZA		Electrochemical reduction of CCl <sub>4</sub>	[40]
Copper net	HKUST-1		Gas separation	[75]
SAMs on Au	HKUST-1	LPE method	Sorption	[76]
FTO-coated with thin TiO <sub>2</sub> layer	HKUST-1	LPE method	Electrical conductivity	[77]
SAMs on Au	Zn <sub>4</sub> (dmcapz) <sub>3</sub>	LPE method	Separation	[78]
SAMs on Au	Heterostructured [Cu <sub>2</sub> (L) <sub>2</sub> (dabco)]	LPE method	Separation	[79]
Copper electrode	HKUST-1	Anodic oxidation	Water adsorption	[80]
FTO	Zn-BTC	EPD	Electrocatalysis	[32]
FTO	MOF-5	Reductive electro-synthesis	Not given	[81]
FTO	NU-1000, UiO-66	EPD	Not given	[82]
Zinc plate	Zn <sub>3</sub> (BTC) <sub>2</sub>	Anodic oxidation	Sensing	[83]
Tb foil, Gd foil	Tb(BTC), Gd(BTC)	Anodic oxidation	Sensing	[84]
Fe	MIL-100(Fe)	Anodic oxidation	Vapor separation	[85]
GC	MOF-5	Electrochemical assisted in situ growth	Photoelectrochemical sensor	[86]
SLG/Cu	COF-5	Solvothermal	Not given	[87]
SLG/ITO	ZnPc-PBBA COF	Solvothermal	Not given	[88]
Au	DAAQ-TFP COF	Solvothermal	Not given	[89]
SAMs/Au	MIL-88(Fe)	Diffusion process	Not given	[90]
	HKUST-1			
HOPG	SCOF-IC1	Diffusion process	Not given	[91]
	SCOF-LZU1			
SLG/Cu	polymerized by BTA and PDA	Diffusion process	Not given	[92]
Porous supports	HKUST-1	Secondary growth	Gas separation	[93]
HOPG/Au	COF-1	Secondary growth	Not given	[94]
Au	polymerized by trans-Br <sub>2</sub> I <sub>2</sub> TPP and DBTF	Secondary growth	Not given	[95]
Au	COF-5	Secondary growth	Not given	[96]
Ag	COF-1 and COF-5	UHV polymerization	Not given	[97]
Au	Polymerized by BBBA	UHV polymerization	Not given	[98]
Au	Polymerized by TMC and TPB	UHV polymerization	Not given	[99]
Silicon	ZIF-8	CVD	Not given	[100]

Remarks on abbreviations: CoPIZA contains [5,10,15,20-(4-carboxyphenyl)porphyrin(Co(III)(CoTCPP) units connected by linear trinuclear Co(II)-carboxylate clusters; SAMs: self-assembled monolayers; L = bdc (1,4-benzene dicarboxylate), ndc (1,4-naphthalene dicarboxylate) and NH<sub>2</sub>-bdc (2-amino-1,4-benzene dicarboxylate), dabco = 1,4-diazabicyclo(2.2.2)octane; SLG: single-layer graphene; SCOF: surface-mounted COF; HOPG: highly oriented pyrolytic graphite.

growth in COF films is typically a reversible condensation process. At this point, the surface coverage of COF films can be regulated by controlling the reversible condensation step. This solvothermal controlled process can be navigated specifically, thanks to its reliance on multiple factors such as pressure, temperature, reaction time, and the nature of solvents.

By controlling the solvent mixtures, COF thin films can selectively grow on the patterning SLG surface. Dichtel and co-workers developed this facile strategy to prepare COF (polymerized by Zn octahydroxyphthalocyanine and 1,4-phenylenebis(boronic acid)) thin films selectively on SLG.<sup>[87]</sup> The reason is assigned to the fact that MeOH with a concentra-

tion in excess of 15 equiv. per boronate ester linkage will inhibit the COF formation. On the contrary, 300 equiv. of MeOH per boronate ester can allow the selective growth of COF films on SLG, since SLG adsorbs Pc monomers and/or Pc-PBBA oligomers on its surface where they condense and nucleate subsequent layers. Regarding COF powders, they nucleate in DMA: o-DCB (o-DCB: ortho-dichlorobenzene) upon substrates with no selectivity. Additionally, Dichtel's group developed a slow titration method to solvothermally fabricate COF thin films on Au substrate.<sup>[88]</sup> They found that slow DMF solution mediated titration (over 1 h) of TFP (1,3,5-triformylphloroglucinol) into DAAQ (2,6-dia-minoanthraquinone) at 90 °C can produce

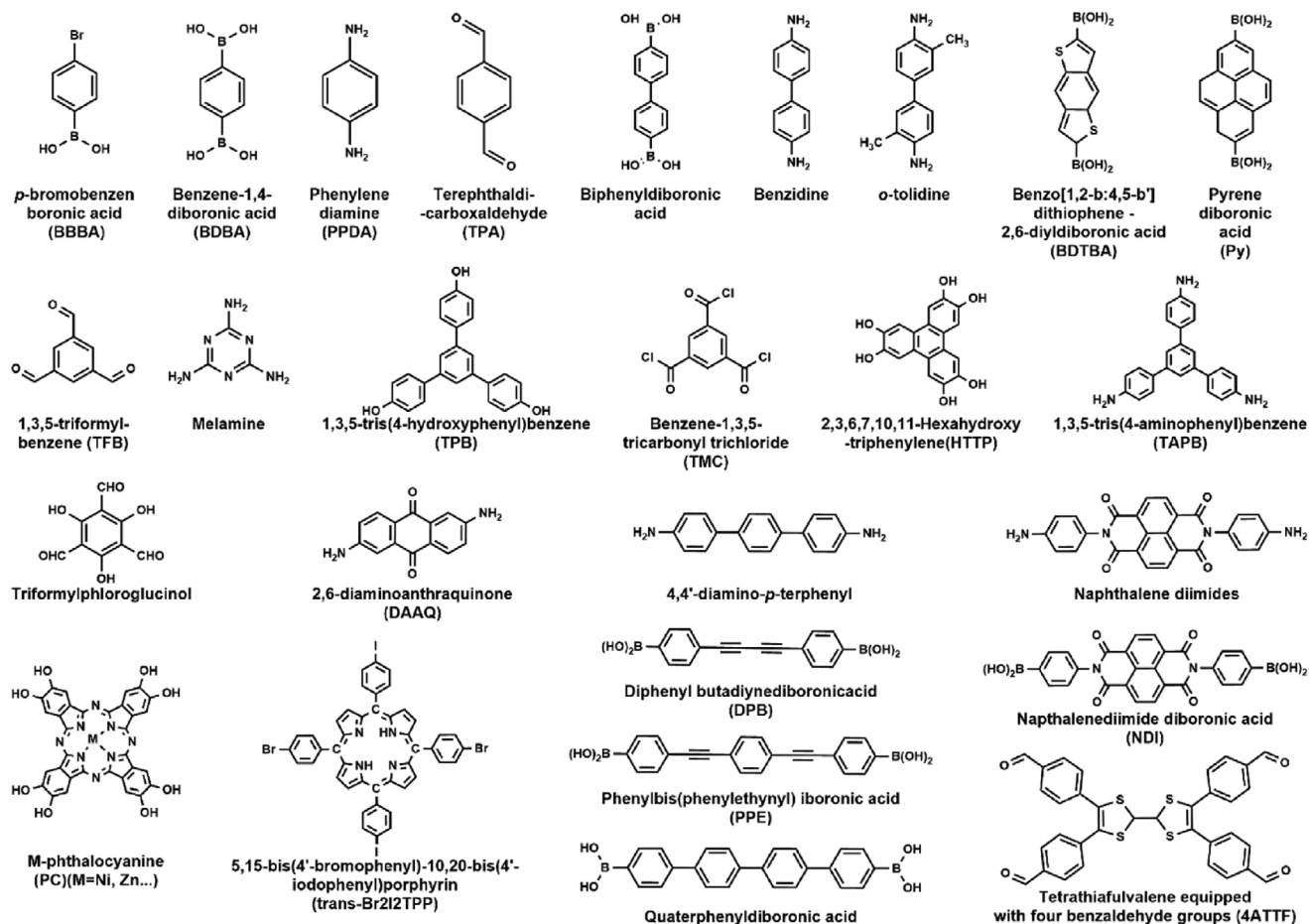
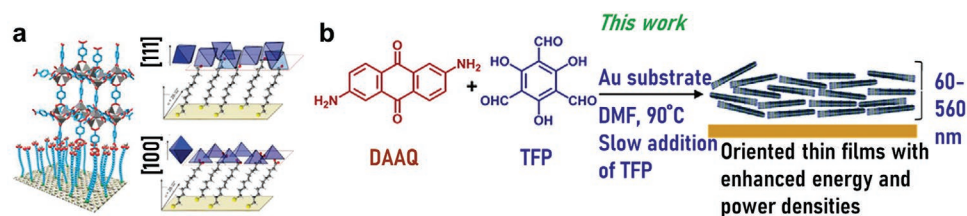


Figure 6. A list of representative monomers used to deposit COF thin films, discussed herein.

Table 7. Pros and cons of various OFM deposition methods listed above.

OFM deposition methods	Pros	Cons
Solvothermal method	Easy and direct	1. Lack of control in preparing a homogeneous thin film; 2. possible substrate corrosion.
LPE LBL method	1. High uniformity; 2. accurate control of film thickness; 3. ultra-thin structures	1. Need for surface functionalization; 2. LBL steps that may need long processing time; 3. only applicable to limited OFMs.
Electrochemical method	1. Enables continuous production; 2. substrate pre-treatment is not necessary; 3. fast reaction process; 4. mild reaction conditions; 5. real-time monitoring of deposition processes.	1. Metal ions with high inertness could separate on the cathode while the organic linkers are possible to be oxidized; 2. the use of heavy metals is not eco-friendly; 3. only valid to conductive substrates.
Controlled diffusion process	1. High rate; 2. easy operation.	1. Limited to easy surface nucleation OFMs; 2. reliance on the penetrated substrates and the diffusion processes.
Secondary growth method	The films are dense and homogeneous.	In principle, this method is applied to wide-ranging systems. 1. The seeding layers remain in the final OFM films, and can therefore reduce the overall porosity and surface area of the final material; 2. the nanoparticles can induce defects into the lattice structures, and this could interfere with the final properties in instances where single crystals are required; 3. if the seeds constitute a problem, customized washing steps might be required to remove any unreacted seed from the final product.
Polymerization under UHV	Uniform and homogenous ultra-thin (monolayer) OFMs.	1. High densities of topological defects can result, thus impeding any long-range order from being introduced. 2. the highly expensive ultra-high vacuum equipment limit their scopes for further translation into myriad applications.
CVD methods	1. Feasibility of controlled patterning; 2. controllable thickness (including ultra-thin variants); 3. uniform, high-aspect ratios.	1. Specific CVD set-up needed; 2. time-consuming search for optimized deposition conditions.



**Figure 7.** a) The concept of depositing MOFs on SAM modified conductive surfaces. Reproduced with permission.<sup>[73]</sup> Copyright 2005, American Chemical Society. Reproduced with permission.<sup>[74]</sup> Copyright 2007, American Chemical Society. b) Solvothermal condensation of HHTP and PBBA in the presence of a substrate-supported SLG surface provides COF-5 as a film on the graphene surface, also as a powder precipitated at the bottom of the reaction vessel. Reproduced with permission.<sup>[89]</sup> Copyright 2015, American Chemical Society.

crystalline and oriented films. The titration pathway can control the polymerization kinetics to optimally afford crystalline films. Thickness of the as-prepared COF thin films can also be controlled by varying the initial monomer concentrations.

Although it is easy and straightforward to use solvothermal method to fabricate MOF thin films on SAM@gold or SAM@FTO glass, it is difficult to solvothermally deposit MOF films on bare conductive substrates due to the weak adherence between the two. Moreover, solvothermal method is time- and energy-consuming. Under solvothermal conditions, precise control of the film thickness poses a challenge, while the thickness eventually plays a key role in determining the mode/extent of charge transfer during electrocatalysis. Besides, direct solvothermal methods are generally handicapped by the lack of control in preparing a homogeneous thin film and also by the possible corrosion of substrates.

### 3.2. OFM Films Obtained via LPE

LPE is another facile method used to deposit OFMs on SAM functionalized conductive substrates.<sup>[103,104]</sup> Regarding MOFs, it is well known that most MOFs are composed of carboxylate and/or N-donor linkers coordinated to metal ions or metal clusters. Therefore, upon exposure to a metal precursor solution, functional groups (e.g., COOH-terminated, pyridine-terminated, and OH-terminated) would first bind to the metals by coordination bonds. Subsequently, pure solvent is used to rinse away the unstable, physically adsorbed metal residues. This ensures a monolayer of metal units to grow on the surface. Afterward, SAM@metal units are immersed in solutions of organic linker(s). The metal units are supposed to coordinate to the organic linkers to afford SAM@MOF layer. A rinsing step hereinafter removes the physically adsorbed units from surface. The surface-exposed, that is, upward-facing functional groups can serve as new reaction sites to trigger the next step of metal precursor deposition. The MOF thin films are finally formed by repeating the above processes. The roughness, homogeneity, and thickness of the MOF thin films can be controlled by adjusting the deposition cycles. Meanwhile, the orientation of these films can be tuned by an exquisite control over the different functional groups pre-modifying the substrate. In general, time spent on the immersion step, reaction temperature and rinsing time are all key factors that contribute to the controlled deposition of films via LPE method. The rational control of reaction time and temperature

can provide MOFs the optimal energy to overcome the kinetic energy barrier and to arrive at a thermal equilibrium. Particularly, an ultrathin MOF film (nm range with a small loading in ng order) can be obtained via LPE method by fine-tuning the fabrication conditions. These established parameters dominate their promising applications in electrolysis. However, LPE method is usually limited to paddle-wheel MOFs. It is still a great challenge to develop LPE to an extent that enables us to fabricate MOFs that feature compositions of higher complexity, such as cage connected MIL-MOFs and porphyrin-MOFs. The possible reason is that under high temperature and high-pressure conditions that would facilitate MOFs to nucleate and grow, it is difficult to exercise control over the LPE fabrication process. For more information, a detailed discussion might be a suitable premise.<sup>[105]</sup> At this point, it is also an imposing challenge to fabricate COFs and other sub-classes of OFMs via LPE, since the formation of covalent bond usually requires high energy to cleave the existing bonds and to then create new bonds. As an exception to this, Tsotsalas and co-workers developed a strategy to fabricate patterning CMP films via orthogonal chemistry.<sup>[106]</sup> First, CMP nanomembranes were prepared based on alkyne-azide cycloaddition (CuAAC) through LBL method. Second, thiol-yne reaction occurred on the surface alkyne, allowing a facile photopatterning of the film surface. However, one drawback of the LPE lies in the lack of control during the crystal orientation along direction(s) parallel to the substrate (in-plane).

### 3.3. OFM Films Obtained via Electrochemical Method

Electrochemical deposition is one of the reported techniques that enables deposition of OFM films directly onto the conductive substrates, especially for the MOF films.<sup>[26]</sup> The prepared OFM thin films are possible to be used as electrocatalysts directly, without post-treatment. It can be divided into four approaches based on the original metal resource: i) Anodic oxidation. The metal ions are produced by anodic oxidation of metal anodes upon applying a certain voltage; while the organic linkers are contained in the electrolytes. Then, the nucleation occurs on the anode surface and grows to form MOF thin films when anodic oxidation continues (**Figure 8a**).<sup>[83,85,108]</sup> ii) Reductive electro-synthesis. Unlike anodic oxidation process, the metal source and organic linkers are both included in the electrolytes. Upon applying a voltage, hydroxide anions are created by electrochemical reduction of water or oxoanions,

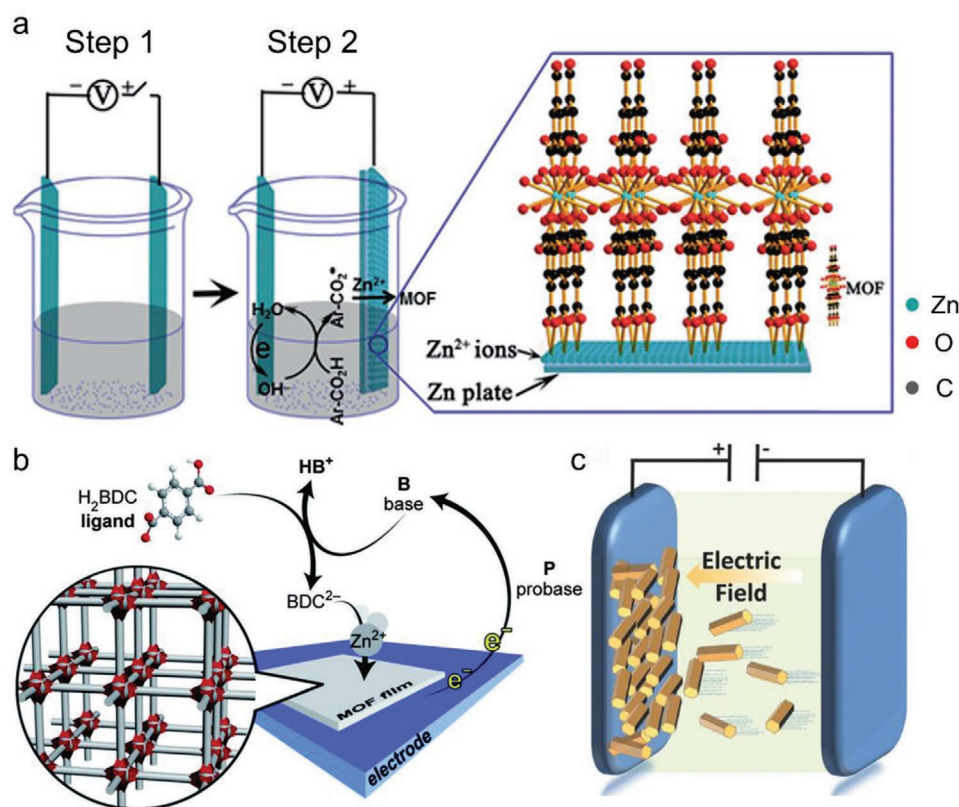


**Figure 8.** Schematic representation of MOFs fabricated via electrochemical deposition methods. a) Reproduced with permission.<sup>[108]</sup> Copyright 2014, Royal Society of Chemistry. b) Reproduced with permission.<sup>[109]</sup> Copyright 2013, Royal Society of Chemistry. c) Reproduced with permission.<sup>[82]</sup> Copyright 2014, Wiley-VCH Verlag GmbH & Co. KGaA, Weinheim.

such as nitrate, which consequently increases solution pH close to the surface and leads to in situ deprotonation of ligands. Subsequently, metal ions near the surface will coordinate to the deprotonated organic linkers to form MOF thin films (Figure 8b).<sup>[109]</sup> iii) Electrophoretic deposition (EPD). Similar to drop-casting post-deposition protocol, EPD requires the suspension of MOF nanoparticles, particularly for electroactive MOFs, into the solution. Subsequently, two conductive electrodes were inserted into the solution and DC electric fields were enforced for driving charged MOF nanoparticles to the conductive surface, thus ending up with MOF thin films (Figure 8c).<sup>[82]</sup> Unlike the drop-casting post-deposition method, EPD can control the homogeneity and thickness by adjusting the applying field and deposition time. However, this method is only available on the structures with electroactive and stabilized electric fields. iv) Galvanostatic displacement approach. Galvanic displacement immediately occurs when a solution containing a greater noble metal concentration is placed on the surface of a metallic support containing a lower noble metal concentration. Owing to the potential difference amongst them, the noble metal is plated on the substrate.<sup>[107]</sup> In this case, the original metal plates are oxidized to yield metal ions, which would further coordinate to organic linkers to afford MOF thin films. This method can produce metal ions locally by in situ galvanic displacement of an underlying metallic support without the supply of any additional external electric field or voltage. However, that the electrochemical method is only available to fabricate OFMs on conductive substrates impedes its application. Besides, the organic ligands

tend to get oxidized while beyond inert conditions, the metal ions can be separately isolated on the cathode. Nonetheless, the use of heavy metals is arguably harmful to our environment.

Regarding the direct deposition of MOFs onto the conductive substrates to afford thin films, although electrochemical method stands out in terms of its scientific maturity, reports on the application of this method to fabricate covalent OFM films such as, COF films, PAF films, HCP films, and CMP films are only limited to a few. Hiroshi et al. have developed a step-by-step electropolymerization in the monomer technique to grow conjugated polymer wires on an iodine-covered Au(111) surface.<sup>[110]</sup> This investigation suggests the possibility to fabricate covalent bond based OFM films on conductive substrates via electrochemical method. However, the bigger challenge in depositing covalent OFM films is embodied in the need to improve their porosity and crystallinity. In this context, Jiang and co-workers deposited CMP thin films on ITO surface via electropolymerization method.<sup>[111]</sup> Working principle of this method is to use a solution-electrode interface for the simultaneous polymerization and consequent deposition of CMPs on electrodes. However, this method is yet to expand beyond the monomers functionalized with N-substituted carbazole units as electropolymerization groups.

### 3.4. OFM Films Obtained via Controlled Diffusion

The OFMs, crystallized by two components, can also be deposited onto supports via liquid diffusion or vaporization

diffusion. Using this technique, the supported surface endows the OFMs a nest for nucleation and also expedites subsequent film growth. The crystallinity, morphology, and thickness of the OFM films can be tailored by controlling the temperature, precursor concentration, and diffusion time. However, this method is limited to the OFMs that are easy to be surface-nucleated. The liquid diffusion approach usually occurs on the porous diffusion substrates; while the vapor diffusion approach has no strict limitation on the choice of substrates. For example, Bein and co-workers kept one component in the polymer gel layer that aids in MOF formation, whereas the other reaction component was kept in the gel layer. Thanks to their controlled diffusion, a nucleation interface of functionalized SAMs results.<sup>[90]</sup> This gel reservoir approach allows the formation of MOF films without the intervention of multiple alternating immersion of the substrates in reactant solutions.

Concerning covalent OFMs such as COFs, the reaction precursors are required to be sealed in a closed container and heated to certain temperature to overcome the nucleation energy barrier. Wan and co-workers developed a self-limiting solid-vapor interface reaction strategy to fabricate highly ordered SCOFs.<sup>[91]</sup> The coupling reaction was tailored to take place at the solid-vapor interface by vaporizing one precursor (precursor B) to the surface on which the other precursor (precursor A) was drop-casted in advance. During this process, the precursors (A and B) were sealed in a closed reactor equipped with thermodynamic regulation agent,  $\text{CuSO}_4 \cdot 5\text{H}_2\text{O}$ . Upon heating the reactor to a certain temperature, precursor B will vaporize to start packing on the top surface of precursor A. Subsequently, covalent bonds can generate at the interface of solid precursor A and the vapor precursor B, thus yielding COF thin films (**Figure 9**). Besides, Lei and co-workers also developed a facile method to synthesize COF thin films at solid/liquid interfaces at room temperature or under evacuation with moderate heating based on condensation reactions between aromatic Schiff-base coupling on highly oriented pyrolytic graphite (HOPG) surface.<sup>[112]</sup> Furthermore, they also prepared COF thin films on single-layer graphene grown on copper foil (SLG-copper). This is based on surface condensation of benzene-1,3,5-tricarbaldehyde (BTA) and p-phenylenediamine (PDA) under ambient conditions.<sup>[92]</sup> This method can grow large-scale highly ordered bi-component 2D SCOFs with low defect density and large domain size.

Additionally, Bein and co-workers reported the deposition of a series of 2D COF films (e.g., benzodithiophene-based COF, BDT-COF; COF-5, boroxine-based pyrene-COF.) on gold FTO via vapor-assisted conversion method at room temperature.<sup>[113]</sup> To be specific, COF precursors were first dissolved in a mixture of acetone/ethanol. Subsequently, they were drop-casted onto substrates. After this, the substrates with coated layer of COF precursors were placed in a desiccator along with a vessel containing mesitylene and dioxane. Then, the desiccator was kept at room temperature for 72 h to ensure that the drop-casted COF precursor solution was completely converted into the corresponding COFs. As studied by XRD and scanning electron microscopy (SEM), it could be seen that the dense and homogenous COF thin films were achieved via vapor-assisted conversion. Besides, the thickness of the as-prepared COF thin films can be modulated by controlling the precursor concentra-

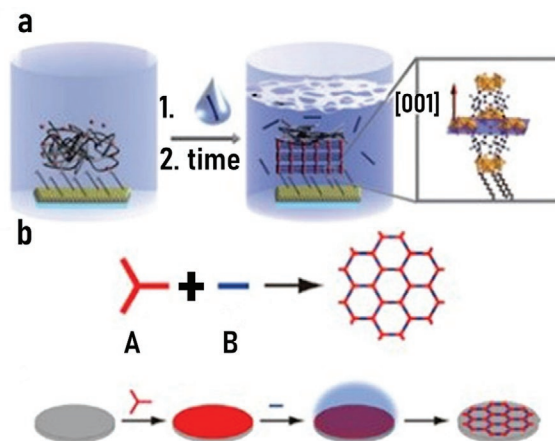


**Figure 9.** a) Representation of the gel-layer approach leading to uniquely oriented nanoscale films of MOFs. A SAM functionalized gold slide is loaded with the metal salt-containing poly(ethylene glycol) gel layer (metal ions shown in red) and covered with a solution containing the linker molecules (shown in blue). Reproduced with permission.<sup>[90]</sup> Copyright 2010, Wiley-VCH Verlag GmbH & Co. KGa, Weinheim. b) Schematic diagram of SCOFs formation: condensation of two precursors A and B featuring different reactive partner groups results in the formation of a typical SCOF. This schematic represents the solid-vapor interface reaction. Reproduced with permission.<sup>[91]</sup> Copyright 2013, American Chemical Society.

tions. However, this approach is only limited to growing COFs that easily nucleate under small amounts of water. For COFs featuring a higher degree of compositional complexity, a facile diffusion method is yet to be developed.

Simply put, to facilitate the growth of OFM films via diffusion of two components placed in a gel reservoir or mother solution or by precursor vaporization, the following criteria need to be met: i) during the conversion of as-prepared MOFs to the corresponding films, building components will not react with the gel layer; whereas for the covalent OFMs, at least one of the precursors can be vaporized under ambient conditions, allowing facile diffusion into the other reactant; ii) easy to nucleate and grow under ambient conditions.

### 3.5. OFM Films Obtained via Secondary Growth

As an alternative route, the OFM nanocrystallites were prepared first to be followed by drop-casting them onto conductive surfaces as layers of nucleation. These grown nuclei were further converted to dense and homogeneous films via secondary solvothermal or tempering treatment.<sup>[93]</sup> In principle, this method applies to a wide variety of OFMs. However, the seeding layers remain in the final OFM films, and can therefore reduce the overall porosity and surface area. The nanoparticles can induce defects into the lattice structure and this could interfere with the final properties in instances where single crystals are required. If the seeds cause an issue, custom-devised washing steps can remove any unreacted seeds from the final product.

A case in point is the work by Lackinger's group where the authors employed boronic acid condensation reaction to deposit

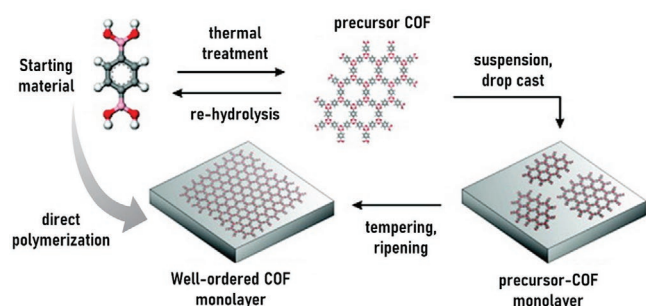


**Figure 10.** Schematic representation of the growth of COF films via sequential reactions guided by the thermal treatment of corresponding precursors. Reproduced with permission.<sup>[94]</sup> Copyright 2011, American Chemical Society.

long-range ordered COF thin films onto a typical graphite surface (Figure 10).<sup>[94]</sup> First, they prepolymerized the monomer into nanocrystalline precursor COFs via thermal treatment. Then, the precursors were drop-casted onto graphite substrates, resulting in the formation of COF thin films with small domain size. This post-synthesis of COF thin films was conducted under relatively ambient conditions, without the use of any expensive UHV and with an optimized time consumption. Besides, formation of the COF thin films counted on reversible reaction conditions, which facilitate long-range order and reduce defects on the surface. Hecht, Grill, and co-workers have developed a strategy for depositing COF films on Au(111) surface by the sequential activation and selection of certain sites (e.g., iodine and bromine) to form covalent bonds in a hierarchical manner.<sup>[95]</sup> In this strategy, 5,15-bis(4'-bromophenyl)-10,20-bis(4'-iodophenyl) porphyrin (Trans-Br<sub>2</sub>I<sub>2</sub>TPP) linkers, which have two bromine and two iodine substituents, were selected. Based on the bond dissociation energies, that is, the difference between bromine-phenyl and iodine-phenyl, (e.g., 336 KJ·mol<sup>-1</sup> for Br-C<sub>6</sub>H<sub>5</sub> and 272 KJ·mol<sup>-1</sup> for I-C<sub>6</sub>H<sub>5</sub> molecules, both in the gas phase), hierarchically built COF films can be realized by stepwise dissociation of two halogen species in the trans-Br<sub>2</sub>I<sub>2</sub>TPP molecules. This occurs in two steps: first, by thermal activation of the iodine sites and then by the subsequent activation of bromine sites at higher temperature. The results show that this pathway allows the fabrication of heterogeneous architectures on Au(111) to endow the film with high electrocatalytic selectivity.

As mentioned above, covalent OFM films are usually obtained by directly placing the substrates in reaction mixtures. However, this approach has demonstrated two major shortcomings: i) COF powders and precipitates result as soon as the thin films form, which would further contaminate them; ii) a variety of monomers and oligomers exist during condensation, which exacerbates the desired control of thickness over the COF thin films. To overcome these limitations, Dichtel developed a novel protocol where COF thin films were deposited on substrates by flowing thermally treated COF precursors. This offers an unmatched control over the film thickness while avoiding contamination by COF powders or the related precipitates (Figure 11).<sup>[96]</sup> The prototypical OFM COF-5, prepared by polymerizing 2,3,6,7,10,11-hexahydroxytriphenylene (HHTP) and 1,4-benzene diboronic acid (BDBA), was chosen as the OFM and the dissolution of monomers in a flow cell was promoted by using a solvent mixture of dioxane/mesitylene, in

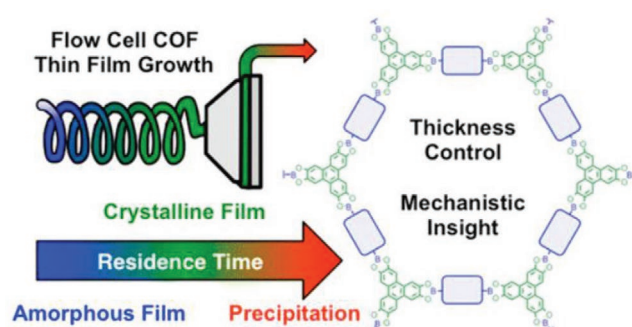


**Figure 11.** Schematic illustrating the growth of COF films via sequential reaction of precursor thermal treatment and flow of mother solution. Reproduced with permission.<sup>[96]</sup> Copyright 2016, American Chemical Society.

presence of a little methanol. Growth of these COF films was conducted via pumping the reaction mixture through a reservoir heated at 90 °C and by subjecting it into a flow cell that comprises a quartz crystal microbalance (QCM) substrate utilized to monitor mass deposition. By monitoring the flow rate, temperature, tube length, and residence time (the period that the monomers are subjected to polymerization before reaching the substrate), and reaction mixture compositions, the mechanism of COF formation can be studied comprehensively. As observed by QCM, the results suggest that this method can offer a superior control over thickness and rates, relative to the other known powder based approaches. But, as to the limitation of the QCM instrument and QCM substrates, only non-corrosive solution and gold based QCM substrates can be used.

### 3.6. OFM Films Obtained via Polymerization under UHV

Unlike the improved level of control achieved over metal-organic interactions, in general, covalently bonded systems are more difficult to control. Therefore, harsh conditions like UHV is desired in most of the covalently bonded OFM thin films. For instance, Abel and co-workers deposited a monomeric layer of COF on Ag(111) surface by subliming BDBA and HHTP under UHV from two heated molybdenum crucible evaporators.<sup>[97]</sup> They obtained SCOF-1 by the intermolecular dehydration of BDBA accompanied by three boronic acid molecules reacting to form a six-membered B<sub>3</sub>O<sub>3</sub> (boroxine) ring with concomitant dehydration. Meanwhile, the condensation reaction of BDBA and HHTP afforded SCOF-2, a dioxaborole heterocycle via an esterification reaction between the boronic acid and the diol groups. Under UHV, the impurities and water molecules produced during condensation get easily removed, resulting in ordered SCOFs with surface coverage ranging from <1% to an extent that implies a near-entire monolayer. Besides the tunable pore size, surface area and high temperature stability of the as-prepared SCOFs can be controlled well. The pore sizes deduced from scanning tunneling microscopy (STM) images are in good agreement with those deduced from DFT calculations. The results indicate that only a small number of defects are formed during the formation of covalent bonds. It also confirms the permanent nature of covalent bonding in the network. In 2012, Abel, Clair, and co-workers developed a number of other SCOFs based on sequential

polymerization with precursor deposition on Au(111) surface under UHV conditions.<sup>[98]</sup> Initially, boronic acid units were polymerized to trimer units, each composed of covalent boroxine rings. Subsequently, C–C bonds between the trimers were formed by thermally activated Ullmann coupling, resulting in the formation of covalent network. The STM studies and DFT calculations indicate that sequential polymerization generate monolayers where nearly all reactive sites of the precursors can successfully engage in covalent bond formation. Gómez-Rodríguez and co-workers employed the prototypal polyester condensation reaction to obtain a defect-free COF thin film on Au(111) surface under UHV condition.<sup>[99]</sup> However, the on-surface condensation polymerizations detailed above are irreversible under UHV; high densities of topological defects can result as an outcome, thus impeding any long-range order from being introduced. High expenses incurred by the ultra-vacuum equipment restrict their wide applications.

### 3.7. OFM Films Obtained via Other Deposition Methods

Alternative methods, such as microwave-induced thermal deposition (MITD),<sup>[114,115]</sup> dip-coating,<sup>[116]</sup> chemical vapor deposition (CVD) methods<sup>[100]</sup> have been developed to fabricate metal-organic OFMs. Regarding MITD, the oft-encountered limitation is that the films are easy to fall off from the substrate due to weak binding interactions between MOF thin films and substrates. As regards the covalently bonded OFMs, it is possible to fabricate them as films via MITD, thanks to the amenability of COFs to this method.<sup>[117]</sup>

Another rather straightforward method to fabricate MOF thin films is to employ dip-coating.<sup>[116]</sup> However, the MOF thin films deposited by this method are not rigidly anchored to the substrate, thus prone to fall thereof. Furthermore, the particle size and roughness cannot be controlled during dip-coating.

In this context, Ameloot and co-workers developed a CVD protocol to deposit MOF thin films with uniform, controlled thicknesses and high-aspect ratios.<sup>[100]</sup> The method consists of two steps. First, a layer of metal oxide was deposited on solid surface via ALD. Second, the ALD metal oxide layers were exposed to an organic linker vapor resulted in a uniform mirror-finish of the highly reflective thin films grown on solid surface. It is possible to fabricate OFMs onto conductive substrates according to the growth mechanism of MOF films formation via CVD. This method can facilitate OFM integration in microelectronic devices which would also be promising in catalytic components.

Regarding other types of PAF thin films, reports of PIM films and HCP films are rare, even more when it comes to their deposition on conductive surfaces. Most research related to PAF, PIM, and HCP films focus on the synthesis of novel structures with various pore sizes that result in gas separation and storage properties. However, it is still a great challenge to find a convenient and low-cost synthesis method to prepare PAF films, PIM films, and HCP films on conductive substrates.

### 3.8. Characterization of OFM Films

Techniques to monitor the growth progress of OFM films and characterizing the as-prepared OFM films are crucial steps for

advancing OFM films into practical applications. Considering the LPE method, growth progress of OFM films on the SAM terminated substrates can be monitored in situ by QCM.<sup>[118]</sup> The frequency change ( $\Delta f$ ) is found to exhibit a linear relationship with the mass adsorbed ( $\Delta m$ ):

$$\Delta m = \frac{c}{n} \Delta f \quad (1)$$

where  $n$  is the harmonic number and  $C$  is a constant for a given QCM instrument. The frequency will change with the change of mass accordingly when the MOF building units rigidly grew on the surface of substrates. In regard to electrochemical deposition, the growth processes can be monitored in situ by modules of a typical electrochemical workstation, such as cyclic voltammetry. Nucleation and phase formation can be clearly deduced from the oxidation/reduction current and potential.<sup>[81]</sup>

Structural conformations, including the growth orientation and their crystallinity can be derived from the grazing-incidence X-ray diffraction (GI-XRD) analysis. Orientations of the OFM on solid surfaces can be examined well by combining in-plane and out-of-plane measurement geometries. Besides, evidences substantiating the linear increase in thickness of OFM films can also be extracted from the XRD data by correlating the XRD line widths (FWHM) with the numbers of deposition cycles. This is done by plotting the deposition cycles versus unit cell number  $N$ . Surface plasma resonance can also be used to study the linear thickness of growth in the OFM films depending on the shift(s) to the refractive indices. Thickness and surface roughness can be directly evaluated by viewing the cross-section and by analyzing the top view of SEM. The cross-sectional view obtained from SEM is only suitable for measuring the samples that feature a clear interface between the OFMs and the substrates. On top of this, scanning force microscopy and/or atomic force microscopy (AFM) can directly be used to measure the thickness and roughness of the as-prepared OFM films. The thickness of MOF thin films can be recorded by a prototypical step profiler.

Reflecting upon the single layer COF films studied thus far, they can be directly imaged using STM and AFM. Pore sizes can be measured directly via the STM and/or AFM images.<sup>[97]</sup> Crystallinity of the aligned COF thin films can be studied by GI-XRD, in which the substrate surface is horizontal and nearly parallel to the incident beam. Coverage and thickness of the films on the surface can be evaluated through AFM or cross-section SEM. X-ray photoelectron spectra can be applied to verify the covalent character of the monolayers.<sup>[94]</sup>

Computational modeling as a complementary tool that delivers understanding the nature and structure of OFMs, is essentially of high repute. Aligned likewise, it is critical to verify the aligned OFM films via theoretical methods. For example, concerning the recently documented SCOF-1 and SCOF-2, it must be verified via a powerful and environment-independent computational tool.<sup>[97]</sup> The authors used density functional theory calculation to validate the recorded experimental data. Agreement between the results obtained from STM measurements and DFT calculations confirm covalent bond formation in the boroxine-linked SCOF-1.

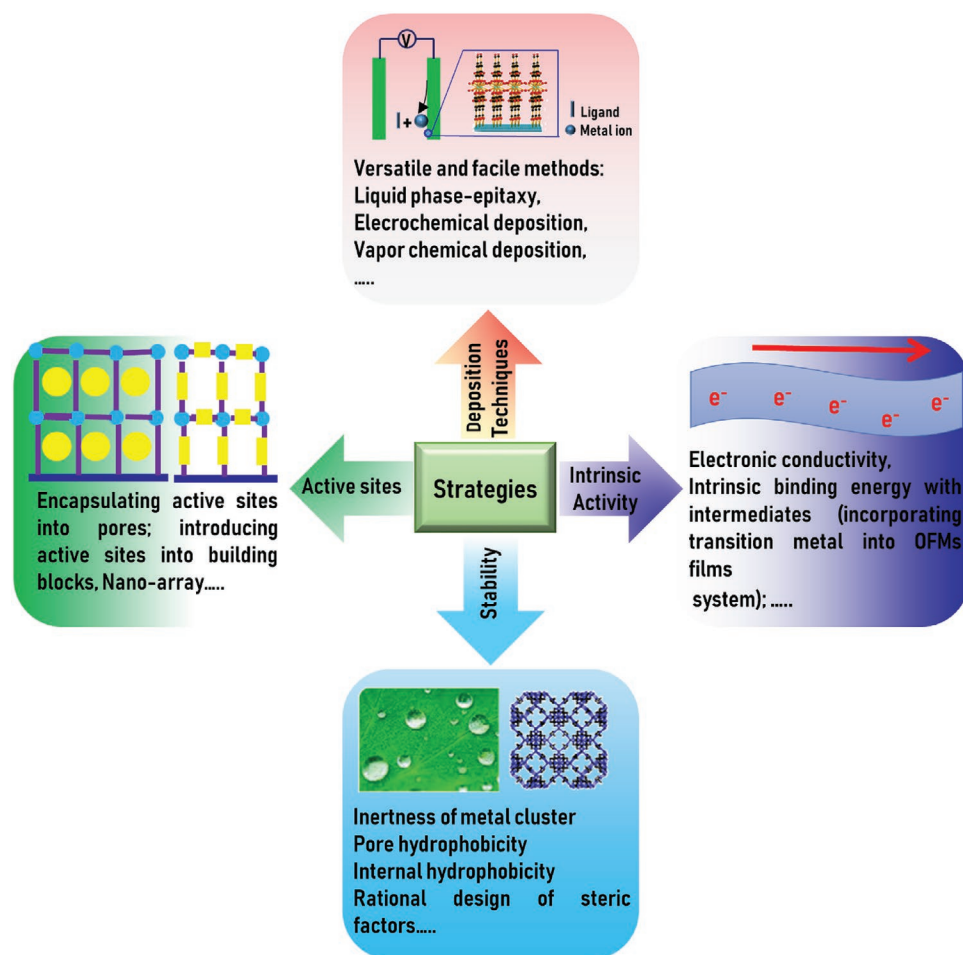


Figure 12. Schematic representation of the developed strategies on OFM films used in electrocatalysis.

#### 4. Developed Strategies on OFM Thin Films Based Energy Materials Used in Electrocatalysis

Many efforts have been invested to develop OFMs for electrochemical energy conversion reactions, especially suitable for reduction or oxidation reaction of  $\text{CO}_2$  and water. But only a few OFM films have demonstrated electrocatalytic performances for the  $\text{CO}_2$  reduction, HER, OER and/or the ORR. The reasons are ascribed to the existing challenges in exploring OFM films for electrocatalysis. For example, the stringent aspects involved in the compatibility between OFMs and conductive substrates, stability of OFM scaffolds, electrical conductivity of OFMs, catalytic active sites configurations, appropriate overpotential, and product selectivity are needed to be critically considered. In the following section, we present our viewpoints on this matter that should, in essence address these foregoing aspects. Besides, the ongoing research efforts on the application of OFM films for electrocatalysis will be examined, especially regarding enhancement of the OFM film stability, increasing the number of active catalytic sites and the intrinsic activity of OFM films in electrocatalysis (Figure 12).

##### 4.1. Strategies to Enhance the Stability of OFM Films in Electrocatalysis

Stability of OFM films primarily rely upon two factors: i) Stability of the OFM skeleton. ii) Compatibility between the OFMs and solid conductive substrates. Both factors are crucial in employing OFM thin films as catalysts. iii) Stability of OFM films as electrocatalysts in electrocatalytic process.

Most OFMs are sensitive to water exposure, typically in vapor (moisture/humidity) and liquid forms. Water molecules are always produced (i.e.,  $\text{CO}_2$  reduction) or needed (i.e., water splitting) during electrocatalytic processes. Thus, understanding the stability of OFMs in the presence of water is of utmost importance for the design and development of OFM films as electrocatalysts. A number of useful reviews have covered the various aspects of MOF stability, including those related to aqueous electrolytes.<sup>[119–123]</sup> Metal-ligand bond strength is regarded as a key indicator to describe the stability of MOFs and is mainly dominated by the Lewis acidity of the coordinated metal nodes and  $\text{p}K_a$  of the linker. The synthesized MOFs will be more stable if they meet the principle of hard and soft acids and bases.<sup>[124]</sup> Other factors, such as the lability of the metal cluster

**Table 8.** Some typical OFMs that are found stable in water and solutions of varying pH.<sup>[125]</sup>

OFMs	Stability	OFMs	Stability
MIL-53 (Al, Fe)	Water; pH, 2–12	MIL-100	Water
PCN-333 (Al, Fe)	Water; pH, 3–9	PCN-333(Cr)	Water; pH, 0–11
PCN-600 (Fe)	Water; pH, 2–11	PCN-426(Cr)	Water; pH, 0–12
PCN-600 (Al)	Water; pH, ≈5	[RE(μ <sub>3</sub> -OH) <sub>8</sub> (1,4-NDC) <sub>6</sub> (H <sub>2</sub> O) <sub>6</sub> ] <sub>n</sub>	Water
Ti(IV) MIL-125	Water	UiO-66, UiO-66 (H <sub>2</sub> N–, Br–, NO <sub>2</sub> -BDC)	Water; pH, 1–7
MOF-808	Water; pH, ≈1	NU-1000	Water; pH, 1–11
ZIF-8	Water; 8 M aqueous NaOH (100 °C)	Ni(BTP)	Boiling water; pH, 2–14
PCN-601	Water; saturated NaOH (100 °C)	PCN-602	Water; saturated NaOH

MIL, Materials of Institute Lavoisier. RE = Eu(III), Tb(III), Y(III), 1, 4-NDC = 1,4-naphthalene dicarboxylate. BTP, 1,3,5-tris(pyrazolate)benzene.

toward water and pH of the solutions, also need to be considered while designing stable, electro-active MOFs. Depending on the interaction strengths of the metal–organic/covalent bonds, OFMs exhibit a varying degree of stability toward water and solution pH (Table 8).<sup>[125]</sup> For example, MOFs built from carboxylate ligands and divalent metals (M<sup>2+</sup>) (e.g., MOF-5, MOF-177, HKUST-1, and MOF-505) are identified as unstable, stemming from the labile nature of metal-carboxylate bonds toward water and acidic/basic solutions.<sup>[122]</sup> Conversely, MOFs such as ZIF-8 and SIM-1 are identified with high water stability across months.<sup>[126]</sup> In solutions of different pH, due to the protonation of organic linker in acidic solution, carboxylate and/or imidazole MOFs were found unstable in acidic media.<sup>[127]</sup> On the contrary, in buffer and alkaline media, BioMOFs and ZIF-8 were reported to be stable.<sup>[128]</sup> For more details on the stability of bulky OFMs toward water and a wider pH range of media, we will guide the readers to other detailed reviews.<sup>[123,129–131]</sup>

To participate in electrocatalytic reactions, the OFMs may need to not only withstand water and the pH changes occurring in solution, but also the operating potentials. During electrochemical operation processes, the building blocks can get reduced or oxidized because of anodic or cathodic polarization. If the building blocks are irreversibly reduced/oxidized and/or strength of the metal–organic bonds are indeed weak across the overpotential window(s), the OFMs may suffer from: i) skeleton collapse, potentially inducing the OFMs to delaminate from the electrode and/or inhibit the accessibility to the substrates and counterions; ii) deactivation of the active sites resulting from a specific component (e.g., the SBUs and/or the organic linkers and/or the metal–organic bonds).<sup>[123]</sup> Recent research from several groups have established that the pristine OFM electrocatalysts could evolve into highly active electrocatalysts via alkaline immersion and/or in situ conversion during the electrocatalytic cycling process.<sup>[51,60,61,132]</sup>

Reflecting upon the above criteria, strategies to design task-specific OFMs with a) high bond strengths of metal–ligand coordination bonds in MOFs and covalent bonds in the other OFMs; b) hydrophobic pores and/or electronic inertness functionalized with exquisitely shielded nodes (e.g., sterically protected metal-oxo clusters or covalent scaffolds in the OFMs). For detailed examples, we direct the readers to the comprehensive literatures.<sup>[122,127,129,133,134]</sup>

Regarding another aspect, compatibility among the OFMs and conductive substrates closely relies upon the thin film fabrication methods. As discussed in Section 3, strengths of the OFMs attached to the conductive substrates are contingent of

the binding force between OFMs and substrate surface. For example, MOF films anchored to the substrate surface with SAMs feature a stronger binding force, when compared to the MOF films that directly grow on surface. 2D COFs are favored considering their deposition on graphene. For a detailed account of OFMs compatible with conductive substrates, we direct readers to a number of useful reviews.<sup>[25,26,135,136]</sup>

#### 4.2. Strategies to Increase the Number of Accessible Active Sites

As discussed in the Section 2, capturing catalytic substrates onto electrocatalyst surfaces, combining and transforming the reaction intermediates and releasing the products are the key steps of the catalytically active sites in driving the electrocatalytic reactions. To deliver the targeted electrocatalytic products, an active site with high efficiency and selectivity must possess an optimal strength of surface adsorption, augmented by formation of the right intermediates whereas the product desorption should be neither too strong nor too weak. An increase in the number of electrically accessible active sites of the catalysts are reckoned with improving the overall electrode activity for the electrocatalytic reactions.<sup>[137]</sup> Consequently it is high-priority to rationally design the catalysts with exposed optimal active sites.

Number of the active sites are often quantified in terms of either mass loading or surface area.<sup>[137]</sup> Accordingly, there are usually two approaches to increase the number of active sites:

- i) by increasing the mass loading of electrocatalysts. In principle, it is comprehensible that the presence of more active sites will boost the overall electrocatalytic activities. Nonetheless, in practice, when catalysts loading increase onto the electrode surface by a certain amount, a limitation is introduced in the mass/charge transport to bring about a plateau effect. The latter impedes any further increase of the overall electrocatalytic activity. Besides, when increasing the mass loading of electrocatalysts, it is also possible that only a small fraction of the active sites contribute to the electrocatalytic reaction, contingent on the electrocatalyst morphology and electrode surface geometry.
- ii) by increasing the surface area of electrocatalysts. That the number of active sites usually depends proportionally on the electrocatalysts surface area controls this aspect. Published reviews and research articles have demonstrated that a wide range of emerging OFMs possess record-high permanent porosity signatures, exemplified by high specific surface

areas.<sup>[138]</sup> Considering MOFs as an example in this regard, porosity of the MOFs can be systematically tailored by pre-selecting the right building blocks (i.e., metal nodes and organic linkers). Besides these traditional design approaches, post-synthetic modifications have also been utilized to regulate the porosity in MOFs. To put it briefly, the intrinsic characteristics of MOFs allow facile optimization of pore sizes and surface areas. But the increase of surface areas in OFMs are indeed associated with their electrocatalytic properties. Currently, multiple promising strategies have been developed to amplify the number of accessible active sites for electrocatalysts:<sup>[51,139]</sup>

- a) Structural engineering. Depositing ultra-thin 2D OFMs (e.g., 2D MOFs and/or 2D COFs) directly onto the electrodes as electrocatalysts could be a potential route to maximize the density of exposed electrocatalytic active sites, thanks to the merits of 2D OFMs with high aspect ratio and the compositional modularity that enables to notch benchmark electrical conductivity by means of controlled active sites.<sup>[140]</sup> Further, by unifying structural engineering with morphology manipulation, fabricating OFM films with vertical alignment, stepped surface structure, hollow structure or nanostructure are also possible, key to maximize the surface-exposed active sites.
- b) Composition engineering. Doping and/or encapsulating the active sites into ordered porous OFM films while retaining their large surface areas is an established approach to enhance the exposure of catalytically active sites.<sup>[31,51,54]</sup>
- c) Substrate engineering. Substrate engineering is defined as the rational selection of conductive substrates for growing OFMs. For example, reports have shown that growing OFMs on the electrodes, such as MXene, N-doped carbon, graphite foam, nickel foam and gas diffusion electrode, can improve the electrocatalytic activity of the OFM films due to an improved density of the exposed active sites and enhanced conductivity.<sup>[54]</sup> Moreover, depositing electrocatalysts on the surface of monolithic supports (e.g., honeycombs, carbon monolith, and foams) as films and/or coatings is also supposed to increase the number of active sites.<sup>[141]</sup> In fact, early studies in monolith structures date back to the 1960s, typically suited for the industrial sector.<sup>[142,143]</sup> Today, monoliths are the preferred support in environment and energy sustainability sectors due to their seamless integration of relevant properties such as easy upscalability, facile orientation in reactors coupled with high degrees of i) temperature durability; ii) surface areas; and iii) mechanical strength.<sup>[144]</sup> The oft-encountered hierarchical porosity in OFMs and OFM@monolith films/coatings are anticipated to result in high density of accessible active sites.<sup>[143,145]</sup>

Although surface area is often used to estimate the number of active sites in electrocatalysts, it must be noted that the measured surface area via gas adsorption (such as, the Brunauer–Emmett–Teller surface area and the Langmuir surface area) tend to overestimate the electrocatalytic surface area. Porosity determined by gas adsorption isotherms do not take into account the electrically neutral surface in a porous solid, routinely causing such discrepancies. To reiterate the obvious, only increasing the number of electrocatalytic active sites via increasing electrochemical surface area can culminate in the development of new electrocatalytic benchmarks, as desired.

### 4.3. Strategies to Increase the Intrinsic Activities of OFM Films

Electron mobility in OFM films is critical in improving kinetic processes and turnover frequencies in electrocatalysis.<sup>[28]</sup> In general, OFM thin films tend to exhibit low electrical conductivity due to their intrinsic low density, mix of metal–organic and/or organic bonds coupled with an ordered arrangement of building blocks (e.g., hard metal ions, carboxyl-based organic ligands, and so on). However, it is important to note that low electrical conductivity does not preclude charge-transfer chemistry upon applied potentials. In fact, a lot of examples of electrocatalysts (e.g., TiO<sub>2</sub>) with low electrical conductivities have been reported thus far.<sup>[146]</sup>

That OFMs often behave as insulators, charge transfer in the OFM films is likely to occur via hopping mechanism. In a typical hopping transport regime, charge carriers such as electrons and holes, reside at specific sites with discrete energy levels and hop between the neighboring sites. The spatial distance ( $R$ ) and the energy difference ( $E$ ) between neighboring hopping sites are dominated by the hopping probability ( $P$ ) (Equation 28,  $\alpha$  is a constant that depends on the nature of hopping sites).

$$P = e^{\left(-\alpha R \frac{E}{kT}\right)} \quad (28)$$

As shown in Equation 28, charge transfer based on a classical hopping mechanism should involve redox sites with the same or similar reduction potentials and isolated immobilized units that are spatially adjacent. Only then, it can ensure that the electrons on the neighboring redox sites can hop efficiently. Thus, the optimization of hopping distance and energy levels between the neighboring hopping sites is a crucial approach to enhance conductivity of the OFMs. So far, charge transport in the reported porphyrin-based OFM thin films used for electrocatalysis can be explained by this hopping mechanism. Adjusting the linker length and/or varying metal nodes that connect neighboring metal porphyrins, electrical conductivities of the OFM films can be improved. For example, COF-366-Co makes use of a direct covalent condensation of 5,10,15,20-tetrakis(4-aminophenyl)porphinato)cobalt with 1,4-benedicarboxaldehyde to exhibit an electrical conductivity in the order of  $\approx 10^{-6}$  S cm<sup>-1</sup>, higher than that of the pristine MOF ( $\approx 10^{-8}$  S cm<sup>-1</sup>). The results show that optimization of covalent bonding can significantly enhance electrical conductivity in prototypical OFM films, such as the above-mentioned COF. For more detail on the role of redox hopping in MOF electrocatalysis, we guide the readers to the feature article.<sup>[147]</sup> Regarding conductivity evaluation on the vast library of currently reported OFMs, we direct the readers to more comprehensive reviews on this subject.<sup>[148,149]</sup>

Apart from the modes of hopping mechanism, charge transfer based on band transport were also proposed to explain the electron transport phenomena occurring in OFM thin films.<sup>[150]</sup> Unlike the regime of hopping transport, charge carriers in the band transport regime are delocalized with effective masses ( $m^*$ ) determined by the band curvature, charger mobility is dominated by the effective mass of the charge carriers and the frequency of charge scattering events (Equation 29,  $\mu$  is the charge mobility,  $e$  is the elemental charge, and  $\tau$  is the mean time between two consecutive charge-scattering events).

$$\mu = \frac{e\tau}{m^*} \quad (29)$$

Nevertheless, both hopping transport and band transport regimes need good spatial and energetic overlaps between the orbitals of appropriate symmetry. Through an increasing orbital overlap, both the charge mobility based hopping and band transport regime can be enhanced. This suggests that creating favorable orbital overlap and facile charge delocalization can generate higher charge mobility, leading to higher conductivities. Depending on the nature of the OFMs, plenty of MOFs exhibit a charge transfer mechanism that involves redox hopping, while COFs follow a band transport mechanism.<sup>[148,151]</sup> During redox hopping, the electrons hop between the electroactive sites and couple with counter-ion diffusion inside the films to preserve the overall electroneutrality of the system. Therefore, ion diffusion is of particular importance to promote the redox hopping of MOF films in electrocatalysis.

In general terms, the prevalent approaches for enhancing conductivity in OFM films include the following strategies (regardless not being restricted to):

- i) Introducing conductive guests (e.g., conductive polymers). For instance, Allendorf and co-workers altered the electrical conductivity of HKUST-1 ( $\text{Cu}_3(\text{BTC})_2$ ,  $\text{BTC}^{3-}$  = benzene 1,3,5-tricarboxylate) from  $10^{-8}$  S  $\text{cm}^{-1}$  (film, four-probe) to 0.07 S  $\text{cm}^{-1}$  by simply incorporating conductive TCNQ molecules into the MOF pores. Calculations of the density of states in TCNQ@HKUST-1 suggests that the lowest unoccupied molecular orbital of TCNQ is close to the valence-band maximum of HKUST-1, resulting in the creation of loosely bound charge carriers between HKUST-1 and the TCNQ molecules. This in turn accelerates electron mobility. Apart from incorporating such conductive guest molecules into the host OFM pores for improving the conductivity, growing OFMs on conductive templates could also be applied to amplify the conductivity of OFMs, due to their orientated facet showing a high propensity for  $\pi$ - $\pi$  coupling with conductive template(s).<sup>[152]</sup>
- ii) Improving electrically conductive properties via structural design of bonding motifs (e.g., metals and ligands). For example, a family of planar 2D MOFs reminiscent of graphite have emerged as promising conductive materials. These 2D MOFs are extended in the form of 2D  $\pi$ -conjugation, thanks to their compositions built from late-transition-metal nodes and oxidized ligands. The late-transition-metal ions and oxidized ligands have widely dispersed valence and conduction bands, implying band transport and thus high charge mobility within the 2D metal-organic sheets.<sup>[153,154]</sup>
- iii) Growing ultrathin (nanometer scale or monolayer) OFM films could also facilitate the electrons transferring through tunneling current. For instance, Sun, Li, and Tang reported the epitaxial growth of a highly oriented 2D MOF on conductive graphene layer.<sup>[152]</sup> Credited to the downsizing of crystal dimension and integration of the conductive template, the prepared 2D MOF shows significant improvement of conductivity suggested by a notably enhanced electrocatalytic performance relative to the MOFs prepared by other exfoliation methods and physically mixed MOFs with 2D conductive templates. The result suggests that fabrication of ultrathin OFM films are possible to promote the electrons transferring through tunneling current.<sup>[155]</sup> Indeed, 2D OFMs have a large lateral size and high aspect ratio, offering various advantages for electrocatalysis.<sup>[156–159]</sup> These are listed as follows:
  - a) Compared to the OFMs of other dimensionality, 2D OFM films exhibit more exposed active sites, often flanked by higher densities.
  - b) Ordered porosity of 2D OFMs enable the diffusion of reactants and products, facilitating the electrocatalytic reaction.
  - c) The ultrathin structures and  $\pi$ -conjugated 2D network structures improve the electrical conductivity and accelerate the charge transport. For instance, Feng, Dong, and co-workers reported a bimetallic layered conjugated MOF, comprising phthalocyaninato copper as the ligand and zinc-bis(dihydroxy) complex ( $\text{ZnO}_4$ ) as the node.<sup>[160]</sup> It demonstrates an improved conductivity that could deliver a high selectivity (88% FE) of electrocatalytic reduction of  $\text{CO}_2$  to CO. Similarly, Dincă and co-workers studied the hierarchical assembly of 2D metal-phthalocyanine (MPc, M = Co or Ni) based MOFs with electrical conductivities of  $2.73 \times 10^{-3}$  S  $\text{cm}^{-1}$  to  $1.04 \times 10^{-1}$  S  $\text{cm}^{-1}$  for electrocatalytic reduction of  $\text{CO}_2$  to CO.<sup>[161]</sup> The results show that the 2D CoPc–Cu–O exhibits the highest selectivity toward CO product ( $\text{FE}_{\text{CO}} = 85\%$ ).
  - d) The modular composition in MOFs and/or MOF derived composites imply the opportunity to tailor the metal ions and/or the organic ligands; moreover, nanoparticles can be loaded in these networks to customize the electrocatalytic activities.

During the initial course of electrons being carried on to the catalyst surface, these are shared with catalysts and the adsorbed guest molecules, leading to the intermediates. As mentioned above, binding ability of the catalysts with specific gases or target molecules dominates the nature of products formed thereafter. Besides, largely because of the kinetic barriers of the adsorbed guest molecules, intermediates, and products, rational design of catalysts with suitable active energy is desired to catalyze various adsorbed guest molecules, translating to useful fuel products. Moreover, selective conversion of the adsorbed guest molecules to specific products demands exclusive catalysts in order to form an intermediate that ends up with the targeted products. Size selectivity imposed by the OFMs can offer great advantages in guiding the selective electrocatalytic conversion of the adsorbed species.

Apart from directly utilizing OFM films for electrocatalysis, incorporating noble metal nanoparticles or late-transition metal nanoparticles into OFM films can also improve the catalytic activities of the OFM films. Despite libraries of nanoparticle loaded OFMs developed for photocatalysis and organic catalysis, to our knowledge, only a limited study exists on nanoparticle-OFM thin films in the context of electrocatalysis.<sup>[162]</sup> LBL method has demonstrated its feasibility in encapsulating nanoparticles and metal oxides into SURMOFs. Thus, it is also possible to deposit active metal nanoparticles onto the OFM films. Besides, electrochemical deposition has also been explored to synthesize mesoporous MOFs. Inspired by this concept, in situ incorporation of active metal nanoparticles and/or active guest molecules into the OFM films is feasible. By elegantly loading nanoparticles onto the OFM films, it could not only enhance the electrocatalytic efficiency, but also improve the conversion selectivity of the adsorbed guest molecules.

Further research for improving the overall electrocatalytic efficiency is under progress by an active pool of electrochemists, materials scientists and engineers in device fabrication, in unison. In this regard, it will be promising to assemble hierarchical OFM films to integrate highly stable, conductive, and

large active sites into one system. Various components are primed to synergistically improve the electrocatalytic efficiency of the resulting scaffolds, on the adsorption of guest molecules to selective generation of products.

#### 4.4. Comparative Studies of OFM Films for Electrocatalytic CO<sub>2</sub> Reduction, Water Splitting, and ORR

As discussed above, stability and the number of accessible electrocatalytically active sites as well as intrinsic characteristics in OFM films are the primary factors that dominate their electrocatalytic activities. A few universal approaches for improving the electrocatalytic activities of OFM films, such as, by enhancing the stability of OFM films, increasing the number of accessible active sites in the OFM films and optimizing the intrinsic activities of the OFM films have been proposed in the preceding sections 4.1–4.3. However, different electrocatalytic reactions demonstrate distinct mechanisms (Tables 1 and 3). For example, electrocatalytic CO<sub>2</sub> reduction shows the possibility of 2e, 4e, 6e, 8e, and/or 12e transfer often accompanied by the reaction media containing DMF, ILs, and aqueous solutions of carbonate salts. While HER and OER is a 2e and 4e transfer reaction, respectively, both often occur in acidic, neutral, or alkaline aqueous solutions. For the ORR, it is a 2e, 4e, or a mixture of 2e and 4e transfer reactions occurring in acidic, neutral, or alkaline aqueous solutions. Therefore, it is crucial to propose strategies beyond the foregoing general ones while

paving ways to design the OFM films for targeted reactions, viz. CO<sub>2</sub> reduction, HER, OER, or ORR, as applicable.

According to the well-known Sabatier principle, the OFM film should possess an optimal binding energy with the intermediates neither too strong nor too weak.<sup>[163]</sup> Consequently, the multi-electron transfer reactions is dominated by the reactions related to the binding strength of the reaction intermediates. These strengths are indicated by the descriptor of a typical volcano plot. To design OFM films for one or more target reaction(s), one could develop new electrocatalysts referring to their customized volcano plot (Figure 13). Furthermore, considering the differences between the reaction media offered by the reactions, the OFM films for various electrocatalytic reactions should sustain the specific reaction conditions. For instance, since the pH of electrolyte solution is higher during the electrocatalytic CO<sub>2</sub> reduction with the consumption of H<sup>+</sup>, the OFM films having a higher alkaline stability are favored for CO<sub>2</sub> reduction. The corresponding OFM films for HER, OER, and ORR are required to exhibit stability in either acid, or neutral, or alkaline medium, respectively.

#### 5. Conclusions and Outlook

The demand for renewable energy and increasing environmental concerns call for the development of new-generation catalysts that enable greener energy conversion reactions. Our review summarizes a thorough analysis of the mechanistic

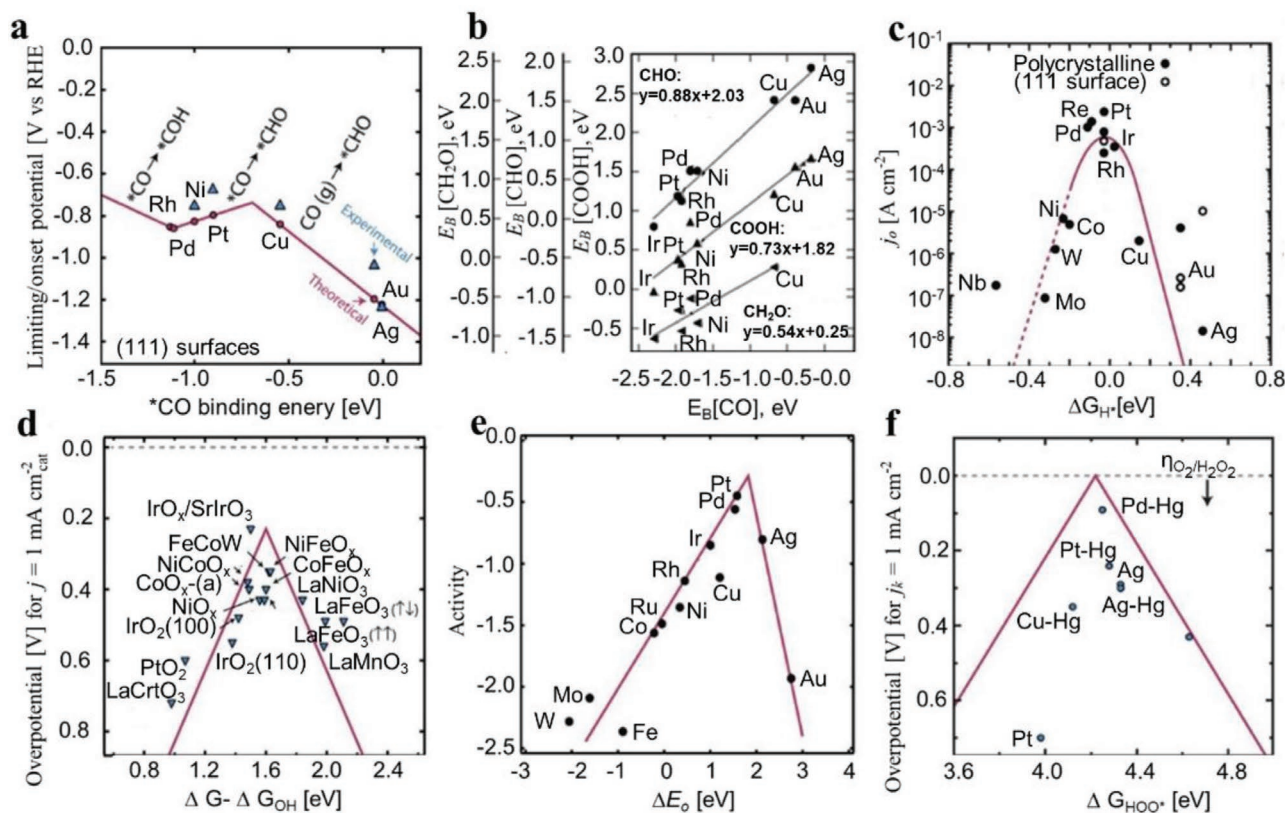


**Figure 13.** Volcano plots for electrocatalytic a,b) CO<sub>2</sub> reduction on metals; c) HER on metals; d) OER on metals; e) ORR on metals; f) H<sub>2</sub>O<sub>2</sub> production on metals and alloys. a,c–f) Reproduced with permission.<sup>[29]</sup> Copyright 2017, American Association for the Advancement of Science. b) Reproduced with permission.<sup>[164]</sup> Copyright 2012, American Chemical Society.

fabrication methods that are likely to sustain OFM films on conductive substrates, including the most recent reports on this topic. A handful of OFM films have been demonstrated as versatile electrocatalysts, particularly in CO<sub>2</sub> reduction, water splitting, and ORR. Electrocatalytic performances in most of the OFM thin films are drawn from the innovatively configured frameworks. However, a systematic mechanistic study of the OFM film assemblies concerning their charge transport mechanisms as well as stabilities in various electrolytes are still essential to assess, in order to demonstrate suitability in electrocatalytic processes. Without such investigations, iterative improvements and adaptations are of great challenge.

A great deal of efforts has been dedicated to integrate OFMs as films onto conductive substrates. Thanks to these conductive substrates, the as-prepared OFM films are amenable to be directly applied under electric fields, especially for electrocatalysis. OFM films have made a worthwhile contribution to the electrocatalysis debate. Cobalt-porphyrin based OFM films in particular, are well-developed for CO<sub>2</sub> electrochemical reduction and OER. Assembling molecules with electrocatalytically active sites into the well-defined and highly ordered frameworks not only avoid the aggregation of porphyrins, but also promote OFM films to expose more active sites. What's more, the permanent porosity of OFMs offer a selective conversion targeted

at specific guest molecules. This intrinsic character also enables to encapsulate highly active nanoparticles with an improved propensity for catalysis. The relatively well-developed deposition methods of OFM films prove that it is indeed feasible to encapsulate highly active nanoparticles into their pores. Diffusion limitation remains a serious hurdle to transport adsorbed guest molecules (i.e., CO<sub>2</sub> and/or water) in catalyzed mediators, and to also desorb the intermediates/products where constricted frameworks are utilized. In this regard, ultrathin OFM films can find utility. Furthermore, further improvements await the conducting OFM films. While at this stage only a few OFMs films have demonstrated electronic conductivity, a rapidly increasing trend is evident.

Besides, OFM thin films can also be employed as precursors to produce a variety of efficient electrocatalysts. Unlike the bulk OFMs, carbonization is often utilized to produce various metal compounds and metal/carbon composites for further electrocatalysis. Direct carbonization of OFM thin films will cause the OFM to get detached from the conductive substrates. Developing mild (pre/post)-treatment methods to prepare a series of MOF film derivatives for advanced electrocatalysts is promising. For example, we recently reported a facile method to prepare highly active electrocatalysts upon immersion of MOF film precursors in alkaline solution (Figure 14).<sup>[60,61]</sup> The studied SURMOF

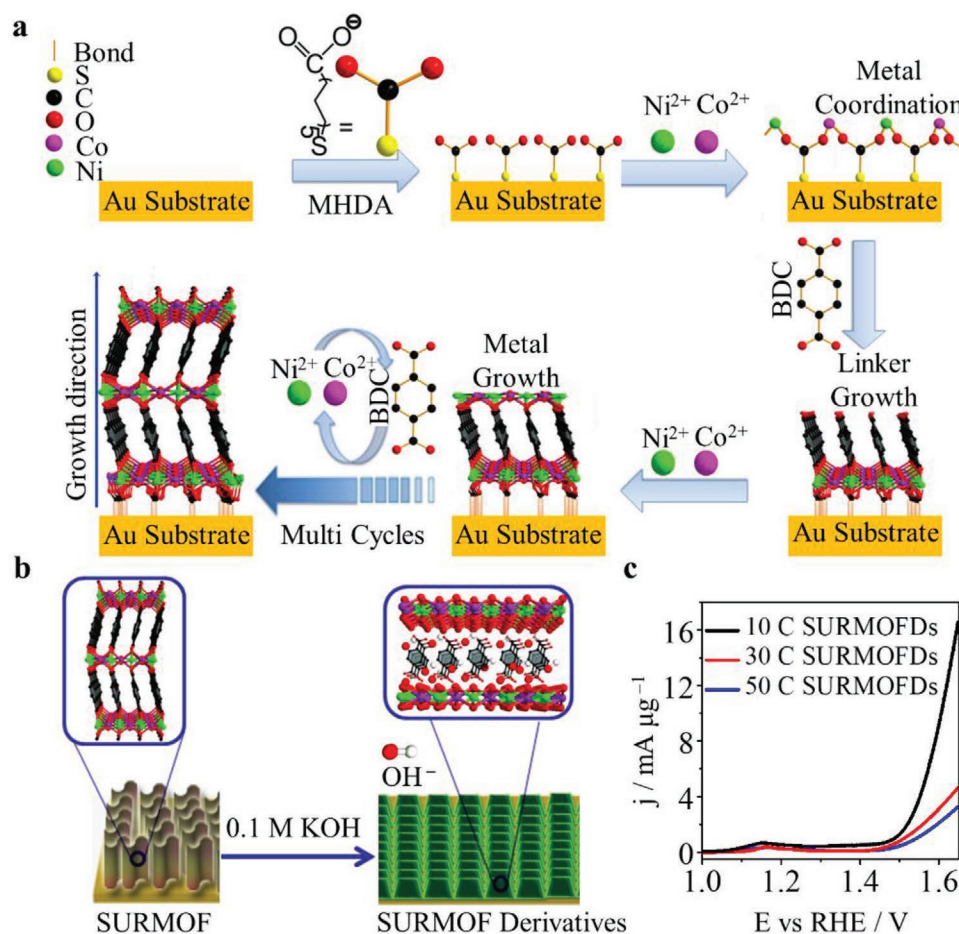


**Figure 14.** Schematic illustrating a) the preparation of SURMOF on gold substrates; b) one-step production of SURMOFDs. c) OER activity of the prepared SURMOF derivatives. (C, cycles). Reproduced with permission.<sup>[60]</sup> Copyright 2019, American Chemical Society.

derivatives show unprecedentedly high  $O_2$  evolution activities with their mass activities  $\approx 3.5$  times higher than any other state-of-art NiFe-, FeCoW-, or NiCo-based electrocatalysts. This high electrocatalytic activity is attributed to the film fabrication and BDC<sup>2-</sup> (H<sub>2</sub>BDC, terephthalic acid) residue interpenetrated structures, which are able to expose the active sites as much as possible. Interestingly, morphology of the SURMOFDs can be tailored by controlling the nucleation (e.g., Ni/Co metal source) and growth (e.g., deposition cycles) process of the SURMOF precursors. By changing the ratio of Ni/Co, morphology of SURMOFDs could be varied from randomly distributed flat nanoplates to homogeneously distributed vertical nanoflakes. The vertical nanoflakes are supposed to expose more accessible active sites and prevent the SURMOFD particles from aggregation. The latter facilitates charge transport, further improving electrocatalytic performance. The tunable deposition cycles enable to tailor the film thickness and assist in improving the charge and/or ion transport. Besides, SURMOFD with different morphologies are anticipated to exhibit distinct roughness and surface areas, resulting in different electrocatalytic performances. Furthermore, by introduction of electron-withdrawing and electron repelling groups to the BDC<sup>2-</sup> linker, a structural lattice strain was induced in the corresponding SURMOFDs, resulting in different morphologies from irregularly distributed particles (-Br), aggregated particles (-OCH<sub>3</sub>), uniform particles (-H) to the vertical nanoflakes.<sup>[61]</sup> Strain modulation in the SURMOFDs results in improvements of bifunctional  $O_2$  reduction and evolution performances with a narrow "overpotential window":  $\Delta E_{ORR-OER}$  of 0.69 V, superior than the benchmark electrocatalysts.

In spite of these significant discoveries, there are still only a handful of OFM films being developed as electrocatalysts. Credited to the nascent stage of this research field, the parameters of OFM films, including electronic conductivity, activation energy, the number of active sites, access density of reactants to the active sites, selectivity of guest molecules and stability, are key contributing factors that need consideration. Keeping these factors in mind, developing OFM thin films on 3D (micro/macro/meso/nano-) porous electrodes, such as 3D gas-diffusion electrode and porous conductive monolith electrode, could potentially improve their exposure of active sites and mass transport. Due to a number of advantages that OFM films offer, it is also promising to develop them in order to target other emerging energy conversion reactions, such as nitrogen reduction reaction ( $N_2 + 6H^+ + 6e^- \rightarrow 2NH_3$ ), hydrogen peroxide production ( $O_2 + 2H^+ + 2e^- \rightarrow H_2O_2$ ), and organic coupling reactions such as C-C bond activation-cum-coupling reactions, to name a few.

Despite their early promises, current research on OFM films continues to focus on lab-scale studies, with only a low benchmark current density of 10 mA cm<sup>-2</sup>. The current density is lagging far behind from the industrial target of 100 mA cm<sup>-2</sup>. Developing electrocatalysts to meet the standards set by industrial sectors, in the forms of high current density, resistance to harsh conditions (e.g., high concentration of alkaline environment and high temperature), is promising for further lab studies. Much progress is still needed on ramping up the electroactivities of OFM films to meet the industrial standards.

## Acknowledgements

W.J.L. is grateful for funding from Sino-Germany (CSC-DAAD) Joint Postdoc Scholarship and Alexander von Humboldt postdoctoral fellowship. S.M. is also thankful to the support of Alexander von Humboldt foundation for postdoctoral fellowship. R.C. and B.H.R. are grateful to NSFC (51572260) and NSFC (22033008).

Open access funding enabled and organized by Projekt DEAL.

## Conflict of Interest

The authors declare no conflict of interest.

## Keywords

covalent organic frameworks, electrochemical catalysis, metal-organic frameworks, open framework materials, thin films

Received: November 5, 2020

Revised: March 2, 2021

Published online:

- [1] J. A. Turner, *Science* **2004**, 305, 972.
- [2] N. S. Lewis, D. G. Nocera, *Proc. Natl. Acad. Sci. USA* **2006**, 103, 15729.
- [3] S. Chu, A. Majumdar, *Nature* **2012**, 488, 294.
- [4] X. Chang, T. Wang, J. Gong, *Energy Environ. Sci.* **2016**, 9, 2177.
- [5] L. Li, J. Yan, T. Wang, Z. J. Zhao, J. Zhang, J. Gong, N. Guan, *Nat. Commun.* **2015**, 6, 5881.
- [6] E. E. Benson, C. P. Kubiak, A. J. Sathrum, J. M. Smieja, *Chem. Soc. Rev.* **2009**, 38, 89.
- [7] J. Gong, L. Zhang, Z.-J. Zhao, *Angew. Chem., Int. Ed.* **2017**, 56, 11326.
- [8] S. Wang, J. Lin, X. Wang, *Phys. Chem. Chem. Phys.* **2014**, 16, 14656.
- [9] G. S. Z. H. Ren, Springer: Berlin/Heidelberg, **2015**.
- [10] T. Ben, S. Qiu, *CrystEngComm* **2013**, 15, 17.
- [11] P. Horcajada, T. Chalati, C. Serre, B. Gillet, C. Sebrie, T. Baati, J. F. Eubank, D. Heurtaux, P. Clayette, C. Kreuz, J. S. Chang, Y. K. Hwang, V. Marsaud, P. N. Bories, L. Cynober, S. Gil, G. Férey, P. Couvreur, R. Gref, *Nat. Mater.* **2010**, 9, 172.
- [12] Y. Bai, Y. Dou, L.-H. Xie, W. Rutledge, J.-R. Li, H.-C. Zhou, *Chem. Soc. Rev.* **2016**, 45, 2327.
- [13] C. S. Diercks, O. M. Yaghi, *Science* **2017**, 355, eaal1585.
- [14] Z. Xiang, D. Cao, *J. Mater. Chem. A* **2013**, 1, 2691.
- [15] S. Mukherjee, M. J. Zaworotko, *Trends Chem.* **2020**, 2, 506.
- [16] T. Ben, H. Ren, S. Ma, D. Cao, J. Lan, X. Jing, W. Wang, J. Xu, F. Deng, J. M. Simmons, S. Qiu, G. Zhu, *Angew. Chem., Int. Ed.* **2009**, 48, 9457.
- [17] N. B. McKeown, P. M. Budd, K. J. Msayib, B. S. Ghanem, H. J. Kingston, C. E. Tattershall, S. Makhseed, K. J. Reynolds, D. Fritsch, *Chem. - Eur. J.* **2005**, 11, 2610.
- [18] C. D. Wood, B. Tan, A. Trewin, H. Niu, D. Bradshaw, M. J. Rosseinsky, Y. Z. Khimyak, N. L. Campbell, R. Kirk, E. Stöckel, A. I. Cooper, *Chem. Mater.* **2007**, 19, 2034.
- [19] J. X. Jiang, F. Su, A. Trewin, C. D. Wood, N. L. Campbell, H. Niu, C. Dickinson, A. Y. Ganin, M. J. Rosseinsky, Y. Z. Khimyak, A. I. Cooper, *Angew. Chem., Int. Ed.* **2007**, 46, 8574.
- [20] M. D. Kärkäs, T. Åkermark, E. V. Johnston, S. R. Karim, T. M. Laine, B.-L. Lee, T. Åkermark, T. Privalov, B. Åkermark, *Angew. Chem., Int. Ed.* **2012**, 51, 11589.
- [21] S. Wang, Y. Hou, S. Lin, X. Wang, *Nanoscale* **2014**, 6, 9930.
- [22] S. Zhao, Y. Wang, J. Dong, C.-T. He, H. Yin, P. An, K. Zhao, X. Zhang, C. Gao, L. Zhang, J. Lv, J. Wang, J. Zhang, A. M. Khattak,

- N. A. Khan, Z. Wei, J. Zhang, S. Liu, H. Zhao, Z. Tang, *Nat. Energy* **2016**, *1*, 16184.
- [23] S. Lin, C. S. Diercks, Y.-B. Zhang, N. Kornienko, E. M. Nichols, Y. Zhao, A. R. Paris, D. Kim, P. Yang, O. M. Yaghi, C. J. Chang, *Science* **2015**, *349*, 1208.
- [24] E. M. Miner, M. Dincă, *Nat. Energy* **2016**, *1*, 16186.
- [25] A. Betard, R. A. Fischer, *Chem. Rev.* **2012**, *112*, 1055.
- [26] W.-J. Li, M. Tu, R. Cao, R. A. Fischer, *J. Mater. Chem. A* **2016**, *4*, 12356.
- [27] C.-W. Kung, S. Goswami, I. Hod, T. C. Wang, J. X. Duan, O. K. Farha, J. T. Hupp, *Acc. Chem. Res.* **2020**, *53*, 1187.
- [28] B. A. Johnson, A. M. Beiler, B. D. McCarthy, S. Ott, *J. Am. Chem. Soc.* **2020**, *142*, 11941.
- [29] Z. W. Seh, J. Kibsgaard, C. F. Dickens, I. Chorkendorff, J. K. Nørskov, T. F. Jaramillo, *Science* **2017**, *355*, eaad4998.
- [30] R. Kortlever, J. Shen, K. J. Schouten, F. Calle-Vallejo, M. T. Koper, *J. Phys. Chem. Lett.* **2015**, *6*, 4073.
- [31] I. Hod, M. D. Sampson, P. Deria, C. P. Kubiak, O. K. Farha, J. T. Hupp, *ACS Catal.* **2015**, *5*, 6302.
- [32] X. Kang, Q. Zhu, X. Sun, J. Hu, J. Zhang, Z. Liu, B. Han, *Chem. Sci.* **2016**, *7*, 266.
- [33] N. Kornienko, Y. Zhao, C. S. Kley, C. Zhu, D. Kim, S. Lin, C. J. Chang, O. M. Yaghi, P. Yang, *J. Am. Chem. Soc.* **2015**, *137*, 14129.
- [34] L. Ye, J. Liu, Y. Gao, C. Gong, M. Addicoat, T. Heine, C. Wöll, L. Sun, *J. Mater. Chem. A* **2016**, *4*, 15320.
- [35] P. D. Luna, W. B. Liang, A. Mallick, O. Shekhah, F. P. G. de Arquer, A. H. Proppe, P. Todorović, S. O. Kelley, E. H. Sargent, M. Eddaoudi, *ACS Appl. Mater. Interfaces* **2018**, *10*, 31225.
- [36] C.-W. Kung, C. O. Audu, A. W. Peters, H. Noh, O. K. Farha, J. T. Hupp, *ACS Energy Lett.* **2017**, *2*, 2394.
- [37] Y. T. Guntern, J. R. Pankhurst, J. Vávra, M. Mensi, V. Mantella, P. Schouwink, R. Buonsanti, *Angew. Chem., Int. Ed.* **2019**, *58*, 12632.
- [38] X. Kang, B. Wang, K. Hu, K. Lyu, X. Han, B. F. Spencer, M. D. Frogley, F. Tuna, E. J. L. McInnes, R. A. W. Dryfe, B. Han, S. Yang, M. Schröder, *J. Am. Chem. Soc.* **2020**, *142*, 17384.
- [39] P. L. Cheung, S. K. Lee, C. R. Kubiak, *Chem. Mater.* **2019**, *31*, 1908.
- [40] S. R. Ahrenholtz, C. C. Epley, A. J. Morris, *J. Am. Chem. Soc.* **2014**, *136*, 2464.
- [41] J. Albo, D. Vallejo, G. Beobide, O. Castillo, P. Castano, A. Irabien, *ChemSusChem* **2017**, *10*, 1100.
- [42] G. Huang, F. Zhang, X. Du, Y. Qin, D. Yin, L. Wang, *ACS Nano* **2015**, *9*, 1592.
- [43] Y. C. Li, Z. Wang, T. Yuan, D.-H. Nam, M. Luo, J. Wicks, B. Chen, J. Li, F. Li, F. P. G. de Arquer, Y. Wang, C. -T. Dinh, O. Voznyy, D. Sinton, E. H. Sargent, *J. Am. Chem. Soc.* **2019**, *141*, 8584.
- [44] X. Wang, Z. Wang, F. P. G. de Arquer, C.-T. Dinh, A. Ozden, Y. C. Li, D.-H. Nam, J. Li, Y.-S. Liu, J. Wicks, Z. Chen, M. Chi, B. Chen, Y. Wang, J. Tam, J. Y. Howe, A. Proppe, P. Todorović, F. Li, T. Zhuang, C. M. Gabardo, A. R. Kirmani, C. McCallum, S. Hung, Y. Lum, M. Luo, Y. Min, A. Xu, C. P. Ó'Brien, B. Stephen, B. Sun, A. H. Ip, L. J. Richter, S. O. Kelley, D. Sinton, E. H. Sargent, *Nat. Energy* **2020**, *5*, 478.
- [45] F. N. Al-Rowaili, A. Jamal, M. S. B. Shammakh, A. Rana, *ACS Sustainable Chem. Eng.* **2018**, *6*, 15895.
- [46] M. C. Luo, Z. Wang, Y. C. Li, J. Li, F. W. Li, Y. Lum, D.-H. Nam, B. Chen, J. Wicks, A. Xu, T. Zhuang, W. R. Leow, X. Wang, C.-T. Dinh, Y. Wang, Y. Wang, D. Sinton, E. H. Sargent, *Nat. Commun.* **2019**, *10*, 5814.
- [47] M. G. Kibria, J. P. Edwards, C. M. Gabardo, C.-T. Dinh, A. Seifitokaldani, D. Sinton, E. H. Sargent, *Adv. Mater.* **2019**, *31*, 1807166.
- [48] C. G. Morales-Guio, L.-A. Stern, X. Hu, *Chem. Soc. Rev.* **2014**, *43*, 6555.
- [49] J. Zhang, Z. Xia, L. Dai, *Sci. Adv.* **2015**, *1*, e1500564.
- [50] N. -T. Suen, S. -F. Hung, Q. Quan, N. Zhang, Y. -J. Xu, H. M. Chen, [51] J. Liu, S. J. Hou, W. J. Li, A. S. Bandarenka, R. A. Fischer, *Chem. - Asian J.* **2019**, *14*, 3474.
- [52] S. Jayabal, G. Saranya, J. Wu, Y. Liu, D. Geng, X. Meng, *J. Mater. Chem. A* **2017**, *5*, 24540.
- [53] S. Roy, Z. Huang, A. Bhunia, A. Castner, A. Gutpa, X. D. Zou, S. Ott, *J. Am. Chem. Soc.* **2019**, *141*, 15942.
- [54] I. Hod, P. Deria, W. Bury, J. E. Mondloch, C.-W. Kung, M. So, M. D. Sampson, A. W. Peters, C. P. Kubiak, O. K. Farha, J. T. Hupp, *Nat. Commun.* **2015**, *6*, 8304.
- [55] D. J. Li, Q.-H. Li, Z. G. Gu, J. Zhang, *J. Mater. Chem. A* **2019**, *7*, 18519.
- [56] C.-W. Kung, J. E. Mondloch, T. C. Wang, W. Bury, W. Hoffeditz, B. M. Klahr, R. C. Klet, M. J. Pellin, O. K. Farha, J. T. Hupp, *ACS Appl. Mater. Interfaces* **2015**, *7*, 28223.
- [57] J. Duan, S. Chen, C. Zhao, *Nat. Commun.* **2017**, *8*, 15341.
- [58] H. X. Jia, Y. C. Yao, J. T. Zhao, Y. Y. Gao, Z. L. Luo, P. W. Du, *J. Mater. Chem. A* **2018**, *6*, 1188.
- [59] L. Wang, Y. Z. Wu, R. Cao, L. T. Ren, M. X. Chen, X. Feng, J. Zhou, B. Wang, *ACS Appl. Mater. Interfaces* **2016**, *8*, 16736.
- [60] W. J. Li, S. Watzelle, H. A. El-Sayed, Y. C. Liang, G. Kieslich, A. S. Bandarenka, K. Rodewald, B. Rieger, R. A. Fischer, *J. Am. Chem. Soc.* **2019**, *141*, 5926.
- [61] W. J. Li, S. Xue, S. Watzelle, S. J. Hou, J. Fichtner, A. L. Semrau, L. J. Zhou, A. Welle, A. S. Bandarenka, R. A. Fischer, *Angew. Chem., Int. Ed.* **2020**, *59*, 5837.
- [62] E. M. Miner, T. Fukushima, D. Sheberla, L. Sun, Y. Surendranath, M. Dincă, *Nat. Commun.* **2016**, *7*, 10942.
- [63] P. M. Usov, B. Huffman, C. C. Epley, M. C. Kessinger, J. Zhu, W. A. Maza, A. J. Morris, *ACS Appl. Mater. Interfaces* **2017**, *9*, 33539.
- [64] R. Dong, M. Pfeffermann, H. W. Liang, Z. K. Zheng, X. Zhu, J. Zhang, X. L. Feng, *Angew. Chem., Int. Ed.* **2015**, *54*, 12058.
- [65] W. Wang, X. Xu, W. Zhou, Z. Shao, *Adv. Sci.* **2017**, *4*, 1600371.
- [66] J. Gascon, F. Kapteijn, *Angew. Chem., Int. Ed.* **2010**, *49*, 1530.
- [67] S. Qiu, M. Xue, G. Zhu, *Chem. Soc. Rev.* **2014**, *43*, 6116.
- [68] S. Eslava, L. Zhang, S. Esconjauregui, J. Yang, K. Vanstreels, M. R. Baklanov, E. Saiz, *Chem. Mater.* **2013**, *25*, 27.
- [69] M. D. Allendorf, R. J. T. Houk, L. Andruszkiewicz, A. A. Talin, J. Pikarsky, A. Choudhury, K. A. Gall, P. J. Hesketh, *J. Am. Chem. Soc.* **2008**, *130*, 14404.
- [70] A. P. Cote, A. I. Benin, N. W. Ockwig, M. O'Keeffe, A. J. Matzger, O. M. Yaghi, *Science* **2005**, *310*, 1166.
- [71] C. J. Doonan, D. J. Tranchemontagne, T. G. Glover, J. R. Hunt, O. M. Yaghi, *Nat. Chem.* **2010**, *2*, 235.
- [72] S. Y. Ding, W. Wang, *Chem. Soc. Rev.* **2013**, *42*, 548.
- [73] S. Hermes, F. Schröder, R. Chelmoski, C. Wöll, R. A. Fischer, *J. Am. Chem. Soc.* **2005**, *127*, 13744.
- [74] E. Biemmi, C. Scherb, T. Bein, *J. Am. Chem. Soc.* **2007**, *129*, 8054.
- [75] H. Guo, G. Zhu, I. J. Hewitt, S. Qiu, *J. Am. Chem. Soc.* **2009**, *131*, 1646.
- [76] O. Zybailo, O. Shekhah, H. Wang, M. Tafipolsky, R. Schmid, D. Johannsmann, C. Wöll, *Phys. Chem. Chem. Phys.* **2010**, *12*, 8092.
- [77] D. Y. Lee, D. V. Shinde, S. J. Yoon, K. N. Cho, W. Lee, N. K. Shrestha, S. -H. Han, *J. Phys. Chem. C* **2014**, *118*, 16328.
- [78] A. Betard, S. Wannapaiboon, R. A. Fischer, *Chem. Commun.* **2012**, *48*, 10493.
- [79] M. Meilikhov, S. Furukawa, K. Hirai, R. A. Fischer, S. Kitagawa, *Angew. Chem., Int. Ed.* **2013**, *52*, 341.
- [80] R. Ameloot, L. Stappers, J. Franssaer, L. Alaerts, B. F. Sels, D. E. De Vos, *Chem. Mater.* **2009**, *21*, 2580.
- [81] M. Li, M. Dincă, *J. Am. Chem. Soc.* **2011**, *133*, 12926.
- [82] I. Hod, W. Bury, D. M. Karlin, P. Deria, C. W. Kung, M. J. Katz, M. So, B. Klahr, D. Jin, Y. W. Chung, T. W. Odom, O. K. Farha, J. T. Hupp, *Adv. Mater.* **2014**, *26*, 6295.
- [83] W. J. Li, S. Y. Gao, Q. H. Li, R. Cao, *J. Mater. Chem.* **2014**, *2*, 19473.
- [84] N. Campagnol, E. R. Souza, D. E. De Vos, K. Binnemans, J. Franssaer, *Chem. Commun.* **2014**, *50*, 12545.

- [85] N. Campagnol, T. Van Assche, T. Boudewijns, J. Denayer, K. Binnemans, D. De Vos, J. Fransaer, *J. Mater. Chem. A* **2013**, *1*, 5827.
- [86] C. Hou, J. Peng, Q. Xu, Z. Ji, X. Hu, *RSC Adv.* **2012**, *2*, 12696.
- [87] J. W. Colson, A. R. Wöll, A. Mukherjee, M. P. Levendorf, E. L. Spittler, V. B. Shields, M. G. Spencer, J. Park, W. R. Dichtel, *Science* **2011**, *332*, 228.
- [88] J. W. Colson, J. A. Mann, C. R. DeBlase, W. R. Dichtel, *J. Polym. Sci., Part A: Polym. Chem.* **2015**, *53*, 378.
- [89] C. R. DeBlase, K. Hernández-Burgos, K. E. Silberstein, G. G. Rodríguez-Calero, R. P. Bisbey, H. D. Abruña, W. R. Dichtel, *ACS Nano* **2015**, *9*, 3178.
- [90] A. Schoedel, C. Scherb, T. Bein, *Angew. Chem., Int. Ed.* **2010**, *49*, 7225.
- [91] X. H. Liu, C. Z. Guan, S. Y. Ding, W. Wang, H. J. Yan, D. Wang, L. J. Wan, *J. Am. Chem. Soc.* **2013**, *135*, 10470.
- [92] L. Xu, X. Zhou, W. Q. Tian, T. Gao, Y. F. Zhang, S. Lei, Z. F. Liu, *Angew. Chem., Int. Ed.* **2014**, *53*, 9564.
- [93] V. V. Guerrero, Y. Yoo, M. C. McCarthy, H. K. Jeong, *J. Mater. Chem.* **2010**, *20*, 3938.
- [94] J. F. Dienstmaier, A. M. Gigler, A. J. Goetz, P. Knochel, T. Bein, A. Lyapin, S. Reichlmaier, W. M. Heckl, M. Lackinger, *ACS Nano* **2011**, *5*, 9737.
- [95] L. Lafferentz, V. Eberhardt, C. Dri, C. Africh, G. Comelli, F. Esch, S. Hecht, L. Grill, *Nat. Chem.* **2012**, *4*, 215.
- [96] R. P. Bisbey, C. R. DeBlase, B. J. Smith, W. R. Dichtel, *J. Am. Chem. Soc.* **2016**, *138*, 11433.
- [97] N. A. Zwaneveld, R. Pawlak, M. Abel, D. Catalin, D. Gimes, D. Bertin, L. Porte, *J. Am. Chem. Soc.* **2008**, *130*, 6678.
- [98] T. Faury, S. Clair, M. Abel, F. Dumur, D. Gimes, L. Porte, *J. Phys. Chem. C* **2012**, *116*, 4819.
- [99] A. C. Marele, R. Mas-Balleste, L. Terracciano, J. Rodríguez-Fernandez, I. Berlanga, S. S. Alexandre, R. Otero, J. M. Gallego, F. Zamora, J. M. Gomez-Rodriguez, *Chem. Commun.* **2012**, *48*, 6779.
- [100] I. Stassen, M. Styles, G. Greci, H. V. Gorp, W. Vanderlinden, S. D. Feyter, P. Falcaro, D. D. Vos, P. Vereecken, R. Ameloot, *Nat. Mater.* **2016**, *15*, 304.
- [101] W. J. Li, S. Y. Gao, T. F. Liu, L. W. Han, Z. J. Lin, R. Cao, *Langmuir* **2013**, *29*, 8657.
- [102] E. L. Spittler, J. W. Colson, F. J. Uribe-Romo, A. R. Woll, M. R. Giovino, A. Saldivar, W. R. Dichtel, *Angew. Chem., Int. Ed.* **2012**, *51*, 2623.
- [103] S. M. Rie Makiura, Yasushi Umemura, Hiroaki Yamanaka, Osami Sakata, Hiroshi Kitagawa, *Nat. Mater.* **2010**, *9*, 565.
- [104] M. Tu, S. Wannapaiboon, R. A. Fischer, *Inorg. Chem. Front.* **2014**, *1*, 442.
- [105] Y. H. Xiao, Z. G. Gu, J. Zhang, *Nanoscale* **2020**, *12*, 12712.
- [106] P. Lindemann, A. Schade, L. Monnereau, W. Feng, K. Batra, H. Gliemann, P. Levkin, S. Bräse, C. Wöll, M. Tsotsalas, *J. Mater. Chem. A* **2016**, *4*, 6815.
- [107] R. Ameloot, L. Pandey, M. Van der Auweraer, L. Alaerts, B. F. Sels, D. E. De Vos, *Chem. Commun.* **2010**, *46*, 3735.
- [108] W. J. Li, J. Liu, Z. H. Sun, T. F. Liu, J. Lu, S. Y. Gao, C. He, R. Cao, J. H. Luo, *Nat. Commun.* **2016**, *7*, 11830.
- [109] M. Y. Li, M. Dincă, *Chem. Sci.* **2014**, *5*, 107.
- [110] H. Sakaguchi, H. Matsumura, H. Gong, *Nat. Mater.* **2004**, *3*, 551.
- [111] C. Gu, N. Huang, Y. Chen, L. Qin, H. Xu, S. Zhang, F. Li, Y. Ma, D. Jiang, *Angew. Chem., Int. Ed.* **2015**, *54*, 13594.
- [112] L. Xu, X. Zhou, Y. Yu, W. Q. Tian, J. Ma, S. Lei, *ACS Nano* **2013**, *7*, 8066.
- [113] D. D. Medina, J. M. Rotter, Y. Hu, M. Dogru, V. Werner, F. Auras, J. T. Markiewicz, P. Knochel, T. Bein, *J. Am. Chem. Soc.* **2015**, *137*, 1016.
- [114] Y. Yoo, H. K. Jeong, *Chem. Commun.* **2008**, 2441.
- [115] W.-J. Li, J.-F. Feng, Z.-J. Lin, Y.-L. Yang, Y. Yang, X.-S. Wang, S.-Y. Gao, R. Cao, *Chem. Commun.* **2016**, *52*, 3951.
- [116] P. Horcajada, C. Serre, D. Grosso, C. Boissiere, S. Perruchas, C. Sanchez, G. Férey, *Adv. Mater.* **2009**, *21*, 1931.
- [117] N. L. Campbell, R. Clowes, L. K. Ritchie, A. I. Cooper, *Chem. Mater.* **2009**, *21*, 204.
- [118] D. Zacher, K. Yusenko, A. Betard, S. Henke, M. Molon, T. Ladnorg, O. Shekhah, B. Schupbach, T. de los Arcos, M. Krasnopolski, M. Meilikhov, J. Winter, A. Terfort, C. Wöll, R. A. Fischer, *Chem. - Eur. J.* **2011**, *17*, 1448.
- [119] J. B. DeCoste, G. W. Peterson, H. Jasuja, T. G. Glover, Y.-G. Huang, K. S. Walton, *J. Mater. Chem. A* **2013**, *1*, 5642.
- [120] N. C. Burtch, H. Jasuja, K. S. Walton, *Chem. Rev.* **2014**, *114*, 10575.
- [121] K. Meyer, M. Ranocchiari, J. A. van Bokhoven, *Energy Environ. Sci.* **2015**, *8*, 1923.
- [122] J. Canivet, A. Fateeva, Y. Guo, B. Coasne, D. Farrusseng, *Chem. Soc. Rev.* **2014**, *43*, 5594.
- [123] B. D. McCarthy, A. M. Beiler, B. A. Johnson, T. Liseev, A. T. Castner, S. Ott, *Coord. Chem. Rev.* **2020**, *406*, 213137.
- [124] R. G. Pearson, *J. Am. Chem. Soc.* **1963**, *85*, 3533.
- [125] G. Mouchaham, S. Wang, C. Serre, *The Stability of Metal-Organic Frameworks*, Vol. 1 (Eds: H. García, S. Navalón), Wiley-VCH, Weinheim, Germany **2018**.
- [126] S. Aguado, J. Canivet, Y. Schuurman, D. Farrusseng, *J. Catal.* **2011**, *284*, 207.
- [127] C. Volkringer, S. M. Cohen, *Angew. Chem., Int. Ed.* **2010**, *49*, 4644.
- [128] D. Cunha, M. Ben Yahia, S. Hall, S. R. Miller, H. Chevreau, E. Elkaim, G. Maurin, P. Horcajada, C. Serre, *Chem. Mater.* **2013**, *25*, 2767.
- [129] A. J. Howarth, Y. Y. Liu, P. Li, Z. Y. Li, T. C. Wang, J. T. Hupp, O. K. Farha, *Nat. Rev. Mater.* **2016**, *1*, 15018.
- [130] S. Yuan, L. Feng, K. C. Wang, J. D. Pang, M. Bosch, C. Lollar, Y. J. Sun, J. S. Qin, X. Y. Yang, P. Zhang, Q. Wang, L. F. Zou, Y. M. Zhang, L. L. Zhang, Y. Fang, J. Li, H. C. Zhou, *Adv. Mater.* **2018**, *30*, 1704303.
- [131] M. Ding, X. Cai, H.-L. Jiang, *Chem. Sci.* **2019**, *10*, 10209.
- [132] W. Zhang, M. Liu, L. Y. S. Lee, *ACS Catal.* **2020**, *10*, 81.
- [133] S. Mollick, S. Mukherjee, D. Kim, Z. Qiao, A. V. Desai, R. Saha, Y. D. More, J. Jiang, M. S. Lah, S. K. Ghosh, *Angew. Chem., Int. Ed.* **2019**, *58*, 1041.
- [134] S. Mollick, S. Mukherjee, D. Kim, Z. W. Qiao, A. V. Desai, R. Saha, Y. D. More, J. W. Jiang, M. S. Lah, S. K. Ghosh, *Angew. Chem., Int. Ed.* **2019**, *58*, 1041.
- [135] O. Shekhah, J. Liu, R. A. Fischer, C. Wöll, *Chem. Soc. Rev.* **2011**, *40*, 1081.
- [136] D. Bradshaw, A. Garai, J. Huo, *Chem. Soc. Rev.* **2012**, *41*, 2344.
- [137] J. D. Benck, T. R. Hellstern, J. Kibsgaard, P. Chakthranont, T. F. Jaramillo, *ACS Catal.* **2014**, *4*, 3957.
- [138] Y. Peng, V. Krungleviciute, I. Eryazici, J. T. Hupp, O. K. Farha, T. Yildirim, *J. Am. Chem. Soc.* **2013**, *135*, 11887.
- [139] J. B. Huang, Y. Jiang, T. Y. An, M. H. Cao, *J. Mater. Chem. A* **2020**, *8*, 25465.
- [140] D. D. Zhu, M. Qiao, J. Liu, T. Tao, C. Guo, *J. Mater. Chem. A* **2020**, *8*, 8143.
- [141] W. M. Carty, P. W. Lednor, *Curr. Opin. Solid State Mater. Sci.* **1996**, *1*, 88.
- [142] V. Tomašić, *Catal. Today* **2007**, *119*, 106.
- [143] J. W. Hou, A. F. Sapnik, T. D. Bennett, *Chem. Sci.* **2020**, *11*, 310.
- [144] R. Nicolas, The Car-engineer online, <http://www.car-engineer.com/cordierite-for-catalytic-converters/>, accessed: Feb, **2021**.
- [145] H. B. Wu, X. W. Lou, *Adv. Sci.* **2017**, *3*, eaap9252.
- [146] M. D. Earle, *Phys. Rev.* **1942**, *61*, 56.
- [147] S. Y. Lin, P. M. Usov, A. J. Morris, *Chem. Commun.* **2018**, *54*, 6965.
- [148] L. S. Xie, G. Skorupskii, M. Dincă, *Chem. Rev.* **2020**, *120*, 8536.
- [149] X. Deng, J. Hu, J. Luo, W. Liao, J. He, *Top. Curr. Chem.* **2020**, *378*, 27.
- [150] X. X. Li, K. Maingan, P. Deria, *Comments Inorg. Chem.* **2018**, *38*, 166.
- [151] H. Kitoh-Nishioka, K. Welke, Y. Nishimoto, D. G. Fedorov, S. Irle, *J. Phys. Chem. C* **2017**, *121*, 17712.

- [152] A. Q. Hu, Q. Q. Pang, C. Tang, J. X. Bao, H. Q. Liu, K. Ba, S. H. Xie, J. Chen, J. H. Chen, Y. Yue, Y. Tang, Q. W. Li, Z. Z. Sun, *J. Am. Chem. Soc.* **2019**, *141*, 11322.
- [153] R. H. Dong, P. Han, H. Arora, M. Ballabio, M. Karakus, Z. Zhang, C. Shekhar, P. Adler, P. St. Petkov, A. Erbe, S. C. B. Mannsfeld, C. Felser, T. Heine, M. Bonn, X. L. Feng, E. Cánovas, *Nat. Mater.* **2018**, *17*, 1027.
- [154] L. Majidi, A. Ahmadiparidari, N. Shan, S. N. Misal, K. Kumar, Z. H. Huang, S. Rastegar, Z. Hemmat, X. D. Zou, P. Zapol, J. Cabana, L. A. Curtiss, A. Salehi-Khojin, *Adv. Mater.* **2021**, *33*, 2004393.
- [155] L. Britnell, R. V. Gorbachev, R. Jalil, B. D. Belle, F. Schedin, M. I. Katsnelson, L. Eaves, S. V. Morozov, A. S. Mayorov, N. M. R. Peres, A. H. C. Neto, J. Leist, A. K. Geim, L. A. Ponomarenko, K. S. Novoselov, *Nano Lett.* **2012**, *12*, 1707.
- [156] C. Wang, Y.-N. Zhao, C.-Y. Zhu, M. Zhang, Y. Geng, Y.-G. Li, Z.-M. Su, *J. Mater. Chem. A* **2020**, *8*, 23599.
- [157] H. Wu, J. Wang, W. Jin, Z. Wu, *Nanoscale* **2020**, *12*, 18497.
- [158] K. Zhao, W. Zhu, S. Liu, X. Wei, G. Ye, Y. Su, Z. He, *Nanoscale Adv.* **2020**, *2*, 536.
- [159] M. D. Zhang, D. H. Si, J. D. Yi, S. S. Zhao, Y. B. Huang, R. Cao, *Small* **2020**, *16*, 2005254.
- [160] H. X. Zhong, M. Ghorbani-Asl, K. H. Ly, J. C. Zhang, J. Ge, M. C. Wang, Z. Liao, D. Makarov, E. Zschech, E. Brunner, I. M. Weidinger, J. Zhang, A. V. Krashennnikov, S. Kaskel, R. H. Dong, X. L. Feng, *Nat. Commun.* **2020**, *11*, 1409.
- [161] Z. Meng, J. M. Luo, W. Y. Li, K. A. Mirica, *J. Am. Chem. Soc.* **2020**, *142*, 21656.
- [162] S. Begum, T. Hashem, M. Tsotsalas, C. Wöll, M. H. Alkordi, *Energy Technol.* **2019**, *7*, 1900967.
- [163] A. J. Medford, A. Vojvodic, J. S. Hummelshøj, J. Voss, F. Abild-Pedersen, F. Studt, T. Bligaard, A. Nilsson, J. K. Nørskov, *J. Catal.* **2015**, *328*, 36.
- [164] A. A. Peterson, J. K. Nørskov, *J. Phys. Chem. Lett.* **2012**, *3*, 251.



**Weijin Li** received his Ph.D. in Fujian Institute of Research on the Structure of Matter, Chinese Academy of Sciences in 2015. Followed a one-year postdoctoral research at the Collaborative Innovation Center of Chemistry for Energy Materials (2011-iChEM) of Xiamen University, he joined Prof. Roland A. Fischer's group at Technical University of Munich as a postdoctoral researcher under the support of Sino-Germany (CSC-DAAD) joint postdoctoral scholarship (2016–2017) and Humboldt Research Fellow (2017–2020). Now, he is a subgroup leader in Prof. R. A. Fischer's group with the research themed on open framework materials films for electrocatalysis and sensors.



**Soumya Mukherjee** received his Ph.D. in Chemistry from the Indian Institute of Science Education and Research, Pune, in 2017. Followed by a 3 years postdoctoral research experience at the Bernal Institute, University of Limerick, Ireland, with Professor Michael J. Zaworotko, Soumya joined Prof. Roland A. Fischer's group at the Technical University of Munich in January 2020, as an Alexander von Humboldt postdoctoral researcher. An awarded member of the Royal Society of Chemistry, and a recipient of the Marie Skłodowska–Curie Actions Individual Fellowships grant (under Horizon 2020), Soumya is keen to develop porous materials for renewable energy and environmental sustainability.



**Baohui Ren** received her bachelor degree from Liaocheng University in 2015. Currently, she is a Ph.D. student at the joint affiliations of the ShanghaiTech University and Fujian Institute of Research on the Structure of Matter (FJIRSM), Chinese Academy of Sciences (CAS), under the supervision of Prof. Dr. Rong Cao (FJIRSM, CAS). Her current research interests focus development of functional porous materials for anti-corrosion application.



**Rong Cao** obtained his Ph.D. from Fujian Institute of Research on the Structure of Matter (FJIRSM), Chinese Academy of Sciences (CAS), in 1993. Following post-doctoral experience in the Hong Kong Polytechnic University and JSPS Fellowship in Nagoya University, he became a professor at FJIRSM in 1998. For his outstanding achievements in the research of chemistry, he won several awards including the “Distinguished young scientists in China (2003)” etc. Now, he is the head of FJIRSM-CAS. His main research interests include supramolecular chemistry, inorganic–organic composite thin films and nanocatalysis.



**Roland A. Fischer** received his Dr. rer. nat. in 1989 and Habilitation in 1995 from Technical University Munich (TUM). He was Associate Professor at Heidelberg University (1996–1997) and Full Professor for Inorganic Chemistry at Ruhr-University Bochum (1997–2015). In 2016, he returned to TUM and took the Chair of Inorganic and Metal-Organic Chemistry. He was elected Vice President of the Deutsche Forschungsgemeinschaft in 2016. He is a member of the European Academy of Sciences. His research focuses on main group 13/transition metal compounds and clusters, precursors for metal-organic chemical vapor deposition, and the materials chemistry of metal-organic frameworks.